scientific reports

OPEN

Investigating the use of green synthesized copper oxide nanoparticles from *Melia azedarach* to combat cadmium stress in wheat

Iram Naz[1], Maryam[1]✉, Aysha Arif Chahel[1]✉, Ishtiaq Ahmad[2], Amber Raza[1], Muhammad Waseem Haider[2], Muhammad Saqlain Zaheer[3]✉, Muhammad Waheed Riaz[4], Muhammad Rizwan[5]✉ & Salim Manoharadas[6]

Wheat (*Triticum aestivum* L.) is a staple crop that is essential for global food security and nutrition. However, cadmium (Cd) stress significantly impairs plant growth and development by disrupting biological processes. This study investigated the potential of the use of CuO nanoparticles synthesized from *Melia azedarach* (MA-CuONPs) as a strategy to mitigate the lethal effects of $CdCl_2$ and enhance the resilience of *T. aestivum* L. cv. Arooj-22. The experiment utilized a completely randomized design with a two-factor factorial arrangement and three replications. The green synthesis of MA-CuONPs was achieved via the use of *M. azedarach* leaves, where copper ions are reduced by plant extracts. The NPs were analyzed via a UV spectrophotometer, which showed a maximum absorbance at 218 nm, confirming the successful formation of green-synthesized MA-CuONPs. The $CdCl_2$ concentrations used were 0, 10, 20, and 30 ppm, whereas MA-CuONPs were applied at concentrations of 0, 10, 15, and 20 ppm. $CdCl_2$ was administered 15 days postgermination, and MA-CuONPs were foliar sprayed during three growth stages, namely, tillering, jointing, and heading, with Tween 80 as a surfactant. The morphological, physiological, and anatomical parameters of the stem and root and yield parameters were recorded and analyzed via Statisticin 8.1 (two-way ANOVA). The results indicated that at the highest Cd concentration (30 ppm), all the measured parameters significantly decreased, reflecting the adverse effects of Cd stress. Conversely, the application of 20 ppm MA-CuONPs significantly increased all the parameters, demonstrating their ability to mitigate Cd-induced stress. As the Cd concentration increased, a corresponding decline in plant performance was observed, while increasing the CuNP concentration led to improved growth and resilience. This study highlights the potential of CuNPs to increase wheat performance under heavy metal stress, positioning them as a promising approach for improving wheat resilience and productivity in contaminated environments.

Keywords Wheat, Cd stress, Arooj-22, MA-CuONPs, Green nanoparticles, *Melia azedarach*, Foliar application, Sustainable agriculture

Wheat (*Triticum aestivum* L.) is among the most commonly grown crops in the world[1]. Wheat is a staple crop consumed in more than 40 countries and provides 82% of the global population with essential protein and calories, with the Food and Agriculture Organization (FAO) predicting that nearly one billion additional tons of grain will be required annually to satisfy the rising demand, as the world's population is projected to reach 9.1 billion by 2050[2]. Wheat is also a primary food grain crop in Pakistan that makes up 72% of the total calories in an average diet[3,4]. It is composed of a large variety of dietary components, including minerals (1.8%), water

[1]Department of Botany, The Government Sadiq College Women University, Bahawalpur, Pakistan. [2]Department of Horticultural Sciences, Faculty of Agriculture and Environment, Islamia University of Bahawalpur, Bahawalpur 63100, Pakistan. [3]Department of Agricultural Engineering, Khwaja Fareed University of Engineering and Information Technology, Rahim Yar Khan, Pakistan. [4]State Key Laboratory of Wheat Breeding, Group of Wheat Quality and Molecular Breeding, College of Agronomy, Shandong Agricultural University, Tai'an 271000, Shandong, China. [5]Institute of Crop Science and Resource Conservation (INRES), University of Bonn, 53115 Bonn, Germany. [6]Department of Botany and Microbiology, College of Science, King Saud University, 11451 Riyadh, Saudi Arabia. ✉email: drmaryam@gscwu.edu.pk; aysha.chahel@gscwu.edu.pk; msaqlainzaheer@gmail.com; m.rizwan@uni-bonn.de

(14%), protein (14%), lipids (2%), crude fiber (22%), and carbohydrates (70%)[5]. It serves multiple purposes and is a key cash crop in Pakistan, contributing 70% to the Rabi season's output and covering 37% of the nation's total cultivated land[5].

Cadmium (Cd), a toxic heavy metal with high mobility and rapid absorption, poses a global health risk, as it contaminates *T. aestivum* by entering the food chain through uptake from the soil into the shoots and roots of edible plants[6,7]. Because of its high bioavailability, Cd is absorbed by plant roots through apoplastic and symplastic pathways, where it is then transported to shoots through the xylem with the aid of transporters and finally to the edible parts via the phloem[8]. Afterward, Cd is transported to the shoot by being loaded into the tracheids or vessel elements of the stele[9]. Cd reduces the biomass and growth of *T. aestivum* and influences the physiological and biochemical functions of the crop[10]. Moreover, Cd toxicity adversely impacts various physiological and metabolic processes, as well as plant development, and the accumulation of Cd in the soil depletes essential resources, ultimately reducing crop yield and fertility[11,12]. Furthermore, the adverse impacts of Cd on plant physiochemical and biological processes gradually impede photosynthesis by lowering stomatal density, restricting the uptake and distribution of nutrients and water, and disturbing vegetative growth and development in wheat[13]. Cd toxicity adversely effects on wheat growth, development and yield. Wheat is very susceptible to Cd toxicity. Cd distresses plant metabolism by hampering nutrient uptake in competition with essential elements, like zinc (Zn), calcium (Ca), and iron (Fe). Cd in wheat tissues brings oxidative stress accompanying that increased the formation of reactive oxygen species (ROS), and damage the lipid peroxidation, and various cellular structures, especially membranes, proteins, and DNA structure[10,13]. Cd toxicity also interrupts the key physiological processes including photosynthesis, respiration and the enzyme activity. It inhibits chlorophyll synthesis and reduces photosynthetic efficiency. Cd can reduce root length, surface area, and whole root biomass for limiting the uptake of nutrients and water. In molecular terms Cd interferes with the hormonal balance and affects growth regulators (auxins and cytokinins) causing stunted growth and retarded development[8,14].

Recent advancements in nanotechnology have revolutionized the research and have thus introduced the potential of engineered nanomaterials to mitigate heavy metal stress in plants[11,13]. It has been reported that copper oxide nanoparticles (CuO NPs) increase plant growth, mitigate oxidative stress, and increase the nutrient acquisition under metal contaminated conditions[11,15]. Due to their capacity to regulate metal homeostasis, promote antioxidant defense systems, and act on rhizosphere interactions, it is reported by many researchers that their use in Cd toxicity reduction is very useful[16]. CuO NPs can change the bioavailability and mobility of Cd in the soil, and subsequently decrease its uptake by plants. It remains unclear how the accumulation, dynamics of transport, and general plant metabolism are affected by the CuO NPs but its use in agriculture crop production can very useful[14,15,17]. The materials known as nanoparticles (NPs) are small, typically less than 100 nm, with different particle sizes, geometries, and features that can be produced on the basis of the particular needs for their application in agriculture[3,18]. Owing to their extremely small size and unique features, crop yield may increase under a range of environmental conditions, and a report states that more than 1300 distinct commercial NPs have been used for many different kinds of potential uses, including agriculture[19,20]. Nanoparticles (NPs) have become unique approach to mitigate the toxicity of Cd[14]. Nanoparticles (NPs) have surfaced as a promising method to mitigate heavy metal stress, particularly Cd toxicity, as they present benefits such as efficient uptake by crop plants, diminished Cd absorption, and improved mineral nutrition, while also strengthening antioxidant defenses, enhancing photosynthetic attributes, and improving anatomical structures and agronomic characteristics in plants impacted by Cd stress[21,22]. The application of plant extracts in green synthesis has recently increased in popularity because these techniques can produce nanoparticles of various sizes and shapes and offer faster preparation rates than microbial methods do, making them especially well-suited for large-scale nanoparticle synthesis[23,24,24]. Because plant extracts contain antioxidants and secondary metabolites that function as biocapping and reducing agents to stabilize the formation of NP crystals, synthesis utilizing these extracts is typically safe, economical, and environmentally friendly[8,18,25].

Foliar application of nanoparticles (NPs) is a promising method for increasing fertilization efficiency in agriculture, as the translocation of NPs through the phloem from leaves is crucial for effective fertilization but is thought to be possible only for NPs smaller than the cell wall pore size exclusion limit of less than 20 nm[26,27]. NPs applied externally can enter the plant through the stomata or the leaf epidermis; after absorption, they may travel via apoplastic or symplastic pathways to reach the vascular tissue. The vascular system, comprising the xylem and phloem, facilitates the distribution of NPs in both upward and downward directions throughout the plant, and NPs are stored primarily in the vacuole and cell wall[18]. Cu nanoparticles play an essential role in the physiology of plants by stimulating defense systems and enzyme activity[18]. CuO NPs are recognized for their low cost, photocatalytic activity, and chemical stability, have enormous potential as anti-infective agents[28,29]. This is due to the large surface area and advantageous crystal shapes[15,18]. CuO NPs increased the contents of photosynthetic pigments and nutrient elements in rice seedlings under Cd stress, promoting growth, especially at low Cd levels. CuO NPs also reduce Cd accumulation by immobilizing it in less harmful forms[9]. CuO NPs improved *T. aestivum* grain and straw yields along with several growth parameters[30].

In the current scenario of increasing environmental degradation, particularly due to heavy metal contamination in soils, there is an urgent need for sustainable solutions. *Melia azedarach*, a plant species prevalent across South Asia, including Pakistan, presents a promising but underexplored solution. This species has potential for both the phytoextraction of cadmium from contaminated soils and the green synthesis of CuO NPs. Investigating the combined use of M. indica for CuO NP synthesis and its application in *T. aestivum* could offer an innovative approach to mitigating Cd uptake in crops, thereby contributing to sustainable agriculture and environmental management.

Materials and methods

Layout and design of the experiment

A pot experiment was conducted to assess Cd stress tolerance in wheat (Arooj- 22) via foliar application of MA-CuONPs at the Botanical Garden of Govt. Sadiq College Women University, Bahawalpur Pakistan. Seeds of the wheat variety Arooj-22 were obtained from the Regional Agricultural Research Institute, Bahawalpur (RARI). The experiment was conducted between November 2023 and March 2024. Pond soil, which was composed of 40% soil and 60% clay, was collected from the nursery. A digital balance was used to weigh 2 kg of sand to put equal amounts into each pot. The pots were measured as follows: their outside diameter was 20 cm, and their height was 18 cm. Wheat (Arroj-22) seeds were carefully washed with distilled water to remove any debris, and *Triticum aestivum* L. wheat seeds were sown in prepared pots. Eight wheat seeds were planted in each individual pot. Plant thinning was performed on the plants at the seedling stage, and 5–6 plants were maintained in each pot until maturity (Fig. 1). In this study, a completely randomized design (CRD) with a two-factor factorial arrangement was employed to investigate the combined effects of CuO NPs and cadmium (Cd) toxicity on wheat plants. In this study, various treatments were used to evaluate the effects of the foliar application of copper nanoparticles on the tolerance of wheat plants to Cd stress. Four Cd concentrations were used: T1, T2, T3, and T4, corresponding to 0 ppm, 10 ppm, 20 ppm, and 30 ppm, respectively. Additionally, the plants were subjected to four different concentrations of copper nanoparticles (L1, L2, L3, and L4) at 0 ppm, 10 ppm, 15 ppm, and 20 ppm. To ensure the reliability of the data, the experiment was replicated three times (R).

Preparation and application of cadmium stress ($CdCl_2$)

To induce Cd stress, wheat plants were subjected to three cadmium chloride ($CdCl_2$) treatments: 0 ppm, 10 ppm, 20 ppm, and 30 ppm. The Cd solution was prepared by dissolving $CdCl_2$ in distilled water at three different concentrations. To prepare 10 ppm Cd, 0.01 g of Cd was dissolved in 1000 mL of distilled water. For 20 ppm Cd, 0.02 g of Cd was dissolved in 1000 mL of distilled water. For 30 ppm Cd, 0.03 g of Cd was dissolved in 1000 mL of distilled water[31]. In total, 3000 mL of distilled water was utilized to prepare the solutions, with 83.33 mL of the solution being applied to each pot (except for the control group). The $CdCl_2$solution was administered via soil irrigation on the 15th day after germination.

Green biosynthesis of copper oxide nanoparticles (CuO NPs)

Fresh leaves of the Chinaberry tree (*Melia azedarach*) were collected from Government Sadiq College Women University, Bahawalpur, Pakistan. The leaves were thoroughly washed to remove dust and dried at room temperature for two weeks. The dried leaves were ground into a fine powder, and 10 g of this powder was dissolved in 250 mL of distilled water. The solution was stirred continuously, heated to 110 °C for 15 min, allowed to cool, and then filtered to obtain the plant extract. A 0.1 M copper sulfate ($CuSO_4$) solution was prepared separately by dissolving 3.9901 g of $CuSO_4$ in 250 mL of distilled water. For the green synthesis of CuO NPs, 85 mL of the prepared $CuSO_4$ solution was mixed with 17 mL of the *Melia azedarach* leaf extract. Upon mixing, the solution changed color from blue to dark green, indicating the reduction of Cu^{2+} ions into stable copper nanoparticles by the bioactive compounds present in the plant extract[31]. The reaction mixture was left undisturbed overnight at room temperature, allowing nanoparticle precipitation. The precipitate was then centrifuged at 10,000 rpm for 10 min, and the resulting pellet was washed 3–5 times with distilled water to remove unreacted components. To ensure proper drying and stabilization, the wet copper nanoparticles were incubated overnight, transferred to an airtight container, and placed in a desiccator to prevent moisture absorption. The green-synthesized CuO NPs, referred to as MA-CuONPs, were stored in Eppendorf tubes containing distilled water and sonicated for 10–15 min to achieve uniform dispersion before further use (Fig. 2). The phytochemicals present in the extract, such as flavonoids and phenolics, contribute to nanoparticle stabilization.

After preparation of Green-synthesized copper oxide (CuO) nanoparticles it's characterization was noticed by using several analytical techniques. Scanning Electron Microscopy (SEM) was used to noticed the surface morphology and size of MA-CuONPs at an accelerating voltage of 80.0 kV and a magnification of 150,000×. Transmission Electron Microscopy (TEM) was used to analyze the internal structure and particle size distribution of MA-CuONPs. Fourier Transform Infrared Spectroscopy (FTIR) (spectra recorded @ 4000–400 cm^{-1} using the KBr pellet method) was done to noticed the functional groups involved in the reduction of MA-CuONPs. X-ray Diffraction (XRD) analysis was done to noticed the crystalline structure and phase composition of

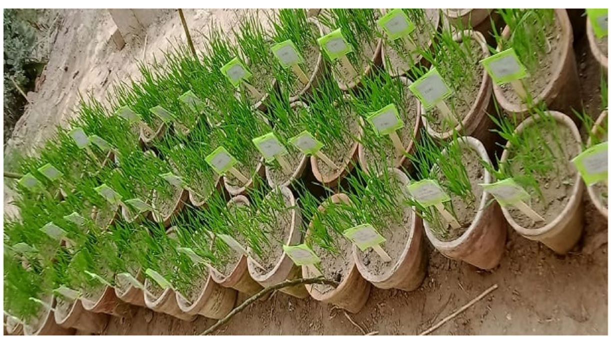

Fig. 1. Wheat plants (Arooj-22) at the experimental site.

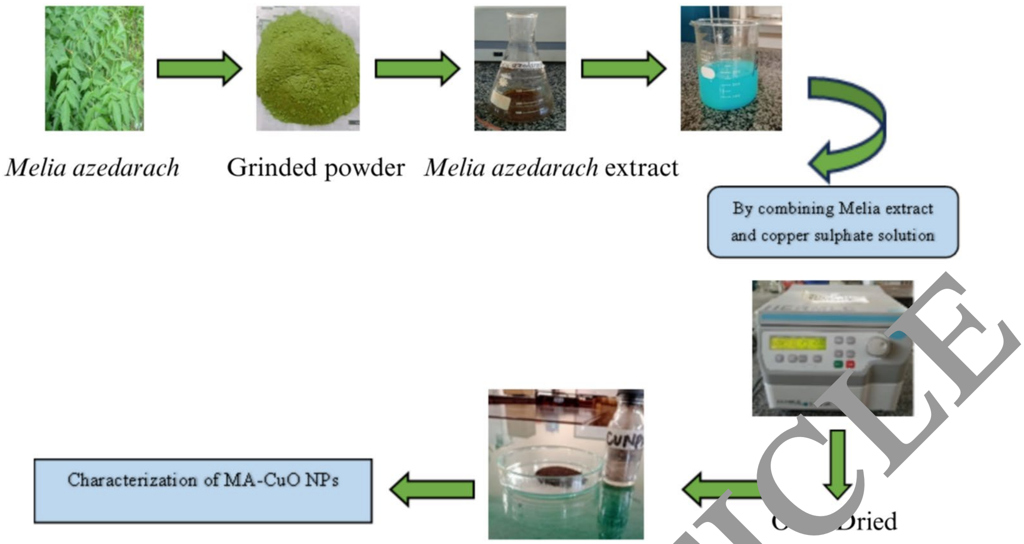

Fig. 2. Schematic diagram of the green synthesis of MA-CuO NPs.

the nanoparticles. The XRD patterns, recorded in the 2θ range of 10° to 70°, that exhibited distinct peaks to monoclinic CuO that can also confirm the successful synthesis of crystalline MA-CuONPs.

Foliar application of MA-CuONP solutions

For foliar application, A prepared solutions of synthesized MA-CuONPs with concentrations of 0 ppm, 10 ppm, 15 ppm and 20 ppm in distilled water were prepared. The 10 ppm MA-CuONPs solution was prepared by the solution of 0.01 g MA-CuONPs in 1000 mL distilled water; 15 ppm and 20 ppm MA-CuONPs solutions were prepared by dissolving 0.015 g, 0.02 g MA-CuONPs in 1000 mL distilled water. 0.1% Tween 80 was added as a wetting and dispersing agent to improve nanoparticle adhesion and minimize runoff loss. In order to prevent the aggregation of nanoparticles and obtain a uniform dispersion, the prepared solutions were sonicated for 15 min[32]. The MA-CuONPs were applied to the wheat leaves by fine mist handheld sprayer in an attempt to achieve fairly even distribution of application. In order to maximize absorption efficiency and minimize evaporation losses, the spraying was carried out in the early morning. The appplication took place at three critical growth stages: first foliar spray was applied when secondary shoots (tillers) appeared on the base of main stem, this corresponded to the early vegetative phase stage. The second spray was used at the onset of fast stem elongation after the first internode appeared, encouraging good plant development. The last foliar spray was applied when wheat inflorescence had emerged well from the sheath and therefore possibility to complement grain filling and stress tolerance. All treatments were applied at the same time of day in order to shade possible treatment effects on time of day and weather. Distilled water combined with Tween 80, but no MA-CuONPs, was applied to control plants. Plant growth parameters, physiological responses and metal accumulation in different plant tissues were monitored to evaluate the effectiveness of foliar applied MA-CuONPs.

Morphological parameters

The morphological data were recorded at the yield stage, specifically when the spikes were fully mature at the grain stage. Plants were randomly selected from each treatment to determine plant height, root length, shoot length, number of leaves, internode length, number of nodes, and total plant fresh and dry weight. The plant height was measured in cm via a measuring tape. The length of each root was recorded from the base of the main root to its tip, also in cm. Shoot length was measured from the base of the main stem to the top of the plant. The number of nodes was counted manually for each treatment. The internode length was measured in cm with a measuring tape. The number of leaves per treatment was counted manually. Wheat plants were carefully removed from the soil, and any soil adhering to the roots was gently wiped off with tissue paper. The plants were then weighed on a digital balance, and their fresh weight was recorded. The total plant dry weight was determined by harvesting the plants and then drying them in an oven at 70 °C overnight. After drying, the dry weight of the plants was measured.

Gaseous exchange parameters

The gas exchange parameters, photosynthetic rate (A), transpiration rate (E), stomatal conductance (gs), intracellular CO_2 (Ci), CO_2 drop, water use efficiency (WUE), and relative water content (RWC) were measured in fully expanded flag leaves at the anthesis stage for each treatment. These measurements were taken between 10:00 a.m. and 11:59 a.m. on a sunny day via an infrared gas analyzer (IRGA) (Long and Bernacchi, 2003)[17,33,34].

Chlorophyll estimation

Fresh wheat leaves (0.5 g) were weighed via an analytical balance and thoroughly washed with distilled water to remove any surface impurities. The washed leaves were finely ground in 80% acetone using a mortar and pestle to extract the chlorophyll pigments. The mixture was then centrifuged at 10,000 rpm for 10 min to separate the chlorophyll extract from the plant debris. The supernatant containing the chlorophyll was carefully collected, and the plant debris was discarded. The chlorophyll extract was washed with distilled water to remove any residual acetone, and the absorbances of the extracts were measured at 480, 645, and 663 nm[35].

$$\text{Chlorophyll (a)} = [(12.7 \times \text{O. D } 663) - (2.69 \times \text{O. D } 645)] \times \text{V}/1000 \times \text{W} \tag{1}$$

$$\text{Chlorophyll (b)} = [(22.9 \times \text{O.D.}645) - (4.68 \times \text{O.D.}663)] \times \text{V}/1000 \times \text{W} \tag{2}$$

$$\text{Total chlorophyllcontent} = [(20.2 \times \text{O.D.}645 + (8.02 \times \text{O.D.}663)] \times \text{V}/1000\ \text{W} \tag{3}$$

$$\text{Carotenoids (Car)} = [\text{O.D } 480 + (0.114 \times \text{O.D } 663)] - (0.638 \times \text{O.D } 645) \tag{4}$$

Where, W is Weight of sample, V is the Volume of extract and O.D. is the Optical Density or Absorbance value recorded using a spectrophotometer at specific wavelengths.

Stem and root anatomy

Fresh, healthy wheat plants were selected from each treatment. Stem sections of 1 cm length were cut from each treatment and carefully sliced into thin sections via a sharp razor blade. The sections were washed in a series of alcohol solutions (30% to 50%) for dehydration and then stained with 1-2 drops of safranin for 1-2 min. Excess stain was removed with 70% and 90% alcohol, and the sections were gently dried using blotting paper. The stained sections were placed on slides, covered with mounting media (glycerin), and sealed with a coverslip. Observations were made at low magnification (4X) for stem length, width, and surface area, followed by higher magnifications (10X and 40X) for detailed examination of stem anatomy, with images captured via a camera-equipped light microscope[36].

Yield parameters

Wheat plants were harvested at the yield stage when the spikes were fully mature. Randomly selected plants from each treatment were analyzed for spike length, number of spikelets per spike, number of grains per spike, spike fresh weight, and spike dry weight. Spike length was measured in cm via a measuring tape. The number of spikelets and grains per spike were counted manually. The spike fresh weight was measured in grams (g) via an analytical balance, and the dry weight was recorded in grams (g) after the spikes were dried overnight in an oven at 70 °C.

Results

Characterization of MA-CuONPs

MA-CuONPs were analyzed via a UV spectrophotometer, and the absorbance was scanned between 200 and 800 nm. The maximum absorbance was observed at 218 nm, indicating the successful presence of green-synthesized MA-CuONPs in the reaction mixture (Fig. 3). Morphology and size of green synthesized CuO nanoparticles derived from *Melia azedarach* extract is showing in the Transmission Electron Microscopy (TEM) image noticed in Fig. 4 (A). Green synthesized CuO nanoparticles shows the spherical and well defined boundaries structure with the diameter of 50 nm. Lattice fringes with an interplanar spacing (d_spacing) of 0.23 nm, confirming their crystalline nature and selected area shows the Electron Diffraction (SAED) pattern showing polycraline nature of this nanoparictle with the presence of concentric diffraction rings. The Scanning Electron Microscopy (SEM) analysis was also conducted at an voltage of 80.0 kV and magnification of 150 k,

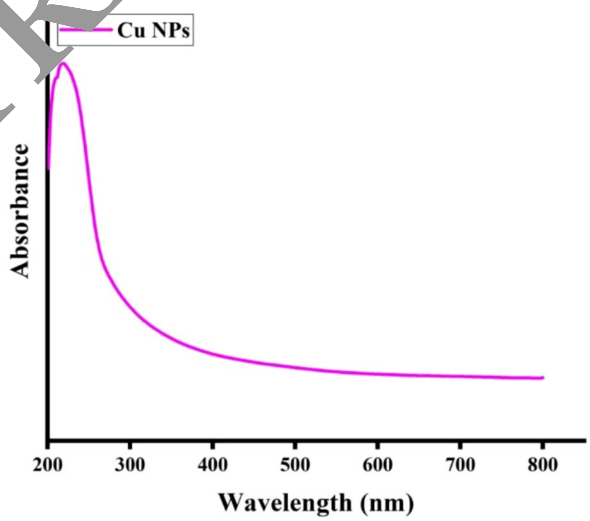

Fig. 3. UV/Vis absorption spectra of MA-CuONPs.

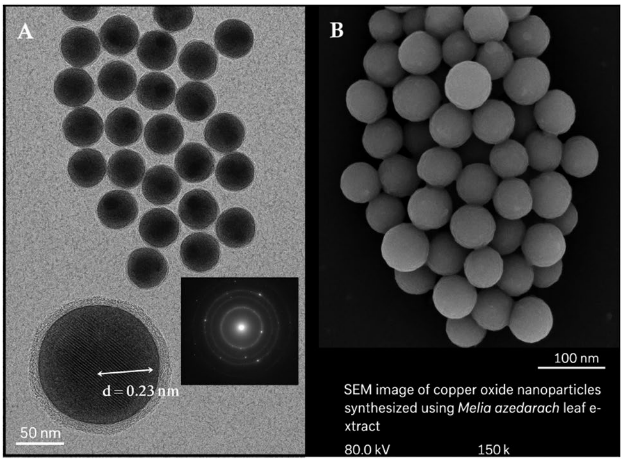

Fig. 4. Crystalline characterization of green synthesized CuO nanoparticles from *Melia azedarach* via TEM (Transmission Electron Microscopy) (**A**) and Scanning Electron Microscopy (SEM) (**B**).

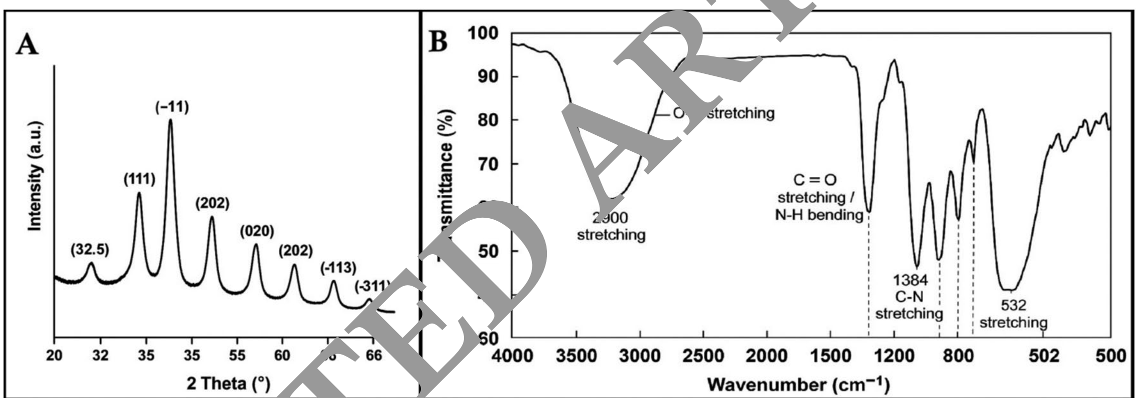

Fig. 5. XRD pattern (**A**) and FTIR spectrum (**B**) of green synthesized copper oxide nanoparticles from *Melia azedarach*.

having the scale representing 100 nm for observation of the structure as noticed in Fig. 4 (B). The smooth surface and the same size distribution shows the effective capping and the stabilization by phytochemicals that also demonstrating the potential of *Melia azedarach* (chinaberry tree) have the reducing and stabilizing agent in the green synthesis protocols. X-ray Diffraction patterm (XRD) of MA-CuONPs shows that the sharp diffraction peaks at 2θ values around 32.5°, 35.5°, 38.7°, 48.7°, 53.5°, 58.3°, 61.5°, 66.2°, and 68.1° correspond to the crystalline planes (32.5), (111), (− 111), (202), (020), (202), (− 113), and (− 311), respectively. Absence of extraneous peaks shows that there was high degree of crystallinity in MA-CuONPs (Fig. 5 A). FTIR spectra of MA-CuONPs show the broad peaks around 3350 cm^{-1}, indicating O–H stretching vibrations. A peak at ~ 1625 cm^{-1} corresponded to C = O stretching of amide linkages, suggesting the involvement of plant proteins in nanoparticle capping. Peaks at 1384 and 1032 cm^{-1} indicated the presence of C–N and C–O functional groups, respectively. A distinct peak at ~ 532 cm^{-1} was confirmed the formation of Cu–O bonds, verifying successful synthesis of CuO nanoparticles (Fig. 5 B).

Cd stress in T. aestivum and mitigation by foliar application of green-synthesized MA-CuONPs

T. aestivum plants were exposed to varying concentrations of cadmium (0 ppm, 10 ppm, 20 ppm, and 30 ppm) and treated with MA-CuONPs at different concentrations (0 ppm, 10 ppm, 15 ppm, and 20 ppm) via foliar application. The effects of these treatments on morphological, physiochemical, gas exchange, and anatomical parameters were evaluated. Morphological data were recorded at the yield stage, specifically when the spikes were fully mature at the grain stage. Gas exchange parameters and chlorophyll content were measured in fully expanded flag leaves at the anthesis stage, while anatomical features were analyzed through cross-sections of relevant tissues.

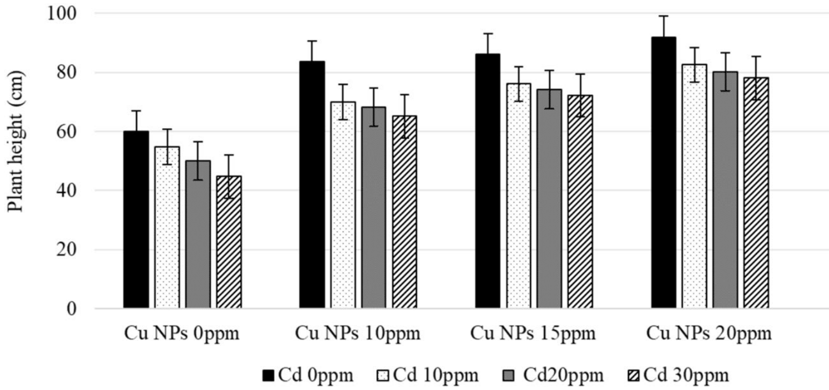

Fig. 6. Impact of different concentrations of Cd and MA- CuO NPs on the plant height of *T. aestivum*.

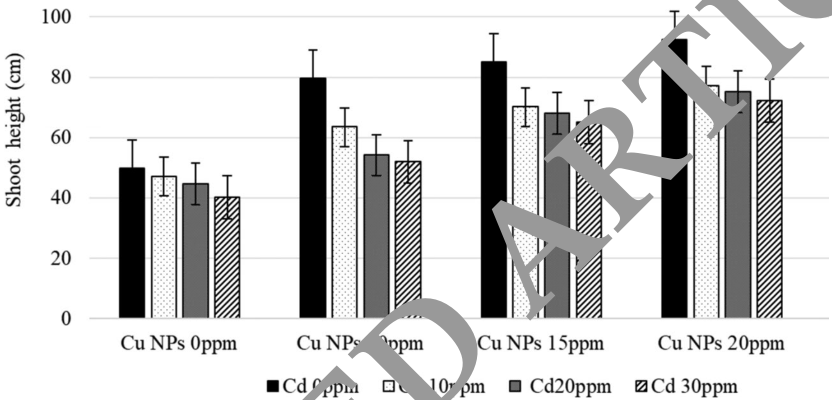

Fig. 7. Impact of different concentrations of Cd and MA- CuO NPs on the shoot height of *T. aestivum*.

Effects of different concentrations of Cd and MA-CuONPs on plant height, shoot length, and root length

The height of *T. aestivum* plants grown with different concentrations of Cd and MA-CuONPs were significantly different among the treatment groups. Under control conditions (0 ppm Cd, 0 ppm MA-CuONP), the plant height was [illegible] cm. Under severe Cd stress (30 ppm, 0 ppm MA-CuONP), the height decreased to 44.73 cm, a 25.6% reduction compared with that of the control, highlighting the negative impact of Cd. Conversely, with 20 ppm MA-CuONPs and no Cd stress, the height increased to 92 cm, a 53% increase from that of the control. The combination of 30 ppm Cd and 20 ppm MA-CuONPs resulted in a height of 78.1 cm, reflecting a 29.9% increase compared with that of the control (Fig. 6). The shoot height of *T. aestivum* grown with different concentrations of Cd and MA-CuONPs is discussed. Under control conditions (0 ppm Cd, 0 ppm MA-CuONP), the shoot height was 49.87 cm. Under severe Cd stress (30 ppm, 0 ppm MA-CuONP), the shoot height decreased to 40.14 cm, representing a 19.5% reduction compared with that of the control, highlighting the negative impact of Cd. Conversely, with 20 ppm MA-CuONPs and no Cd stress, the shoot height increased to 92.4 cm, an impressive 85.1% increase from that of the control. The combination of 10 ppm MA-CuONPs with 30 ppm Cd resulted in a shoot height of 51.93 cm, reflecting a modest 4.2% increase compared with that of the control. Additionally, the application of 15 ppm MA-CuONPs in conjunction with 30 ppm Cd resulted in a shoot height of 65.07 cm, a significant 30.4% increase compared with that of the control (Fig. 7). The root length of *T aestivum plants* grown with different concentrations of Cd and MA-CuONPs also significantly differed among the treatment means. Under control conditions (0 ppm Cd, 0 ppm MA-CuONP), the root length was 3.64 cm. Under severe Cd stress (30 ppm, 0 ppm MA-CuONP), the root length decreased to 2.40 cm, representing a 34.1% reduction compared with that of the control, highlighting the negative impact of Cd. Conversely, with 20 ppm MA-CuONPs and no Cd stress, the root length increased to 4.81 cm, a significant 32.1% increase from that of the control. The combination of 10 ppm MA-CuONPs with 30 ppm Cd resulted in a root length of 3.02 cm, reflecting a 17.1% increase compared with that of the control. Additionally, the application of 15 ppm MA-CuONPs in conjunction with 30 ppm Cd resulted in a root length of 3.26 cm, which was 10.3% greater than that of the control (Fig. 8).

Effects of different concentrations of Cd and MA-CuO NPs on the number of leaves, number of nodes and internodal distance

The number of leaves of *T. aestivum* grown with different concentrations of Cd and MA-CuO NPs was significantly different among the treatment methods. Under the control conditions (0 ppm Cd, 0 ppm MA-CuO

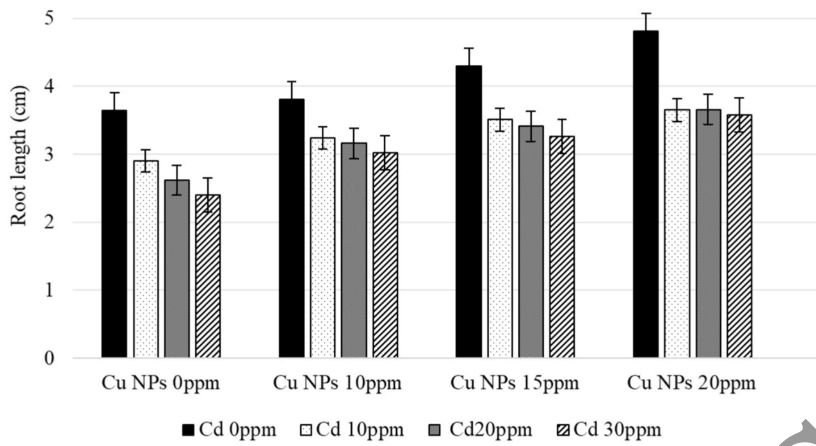

Fig. 8. Impact of different concentrations of Cd and MA- CuO NPs on the root length of *T. aestivum*.

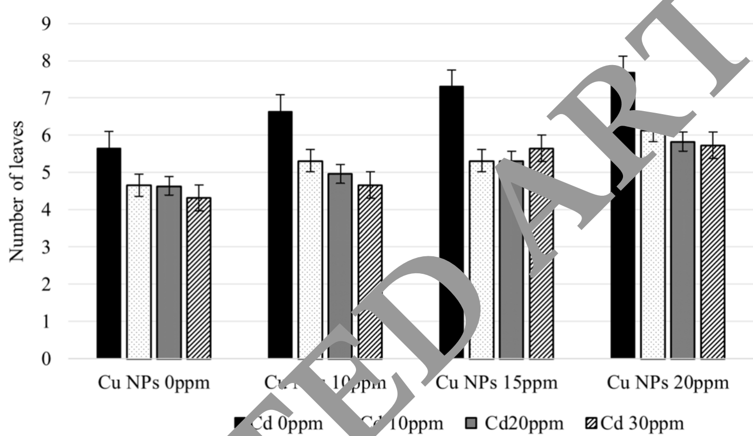

Fig. 9. Impact of different concentrations of Cd and MA- CuO NPs on the number of leaves of *T. aestivum*.

NPs), the number of leaves was 5.65. Under severe Cd stress (30 ppm, 0 ppm MA-CuO NPs), the number of leaves decreased to 4.31, representing a 23.7% reduction compared with that of the control, highlighting the negative impact of Cd. Conversely, with 20 ppm MA-CuO NPs and no Cd stress, the number of leaves increased to 7.68, a significant 35.7% increase from the control. Compared with the control, the combination of 10 ppm MA-CuO NPs with 30 ppm Cd resulted in 4.66 leaves, reflecting a 17.5% increase. Additionally, the application of 15 ppm MA-CuO NPs in conjunction with 30 ppm Cd resulted in 5.64 leaves, showing a modest 0.5% increase compared with the control (Fig. 9). Under control conditions (0 ppm Cd, 0 ppm MA-CuO NPs), the number of nodes was 5.26. Under severe Cd stress (30 ppm, MA-CuO NPs 0 ppm), the number of nodes decreased to 4.33, representing a 17.7% reduction compared with that of the control, highlighting the negative impact of Cd. Conversely, with 20 ppm MA-CuO NPs and no Cd stress, the number of nodes increased to 5.68, a 7.9% increase from the control. Compared with the control, the combination of 10 ppm MA-CuO NPs with 30 ppm Cd resulted in 4.20 nodes, reflecting a 20.1% decrease. Additionally, the application of 15 ppm MA-CuO NPs in conjunction with 30 ppm Cd resulted in 4.75 nodes, indicating a 10.0% decrease compared with the control (Fig. 10). The internodal distance of *T. aestivum* grown with different concentrations of Cd and MA-CuO NPs was investigated. Under control conditions (0 ppm Cd, 0 ppm MA-CuO NPs), the internodal distance was 15.2 cm. Under severe Cd stress (30 ppm, 0 ppm MA-CuO NPs), the internodal distance decreased to 10.2 cm, a 32.9% reduction compared with that of the control, highlighting the negative impact of Cd. Conversely, with 20 ppm MA-CuO NPs and no Cd stress, the internodal distance increased to 17.26 cm, representing a 13.4% increase from the control. The combination of 10 ppm MA-CuO NPs with 30 ppm Cd resulted in an internodal distance of 13.00 cm, reflecting a 14.6% decrease compared with that of the control. The application of 15 ppm MA-CuO NPs in conjunction with 30 ppm Cd resulted in an internodal distance of 14.06 cm, a 7.5% decrease compared with that of the control (Fig. 11).

Effects of different concentrations of Cd and MA-CuO NPs on the fresh and dry weights of the plants

The effects of varying Cd and MA-CuONP concentrations on the fresh weight of *T. aestivum* revealed statistically significant differences among the treatments. Under the control conditions (0 ppm Cd, 0 ppm MA-

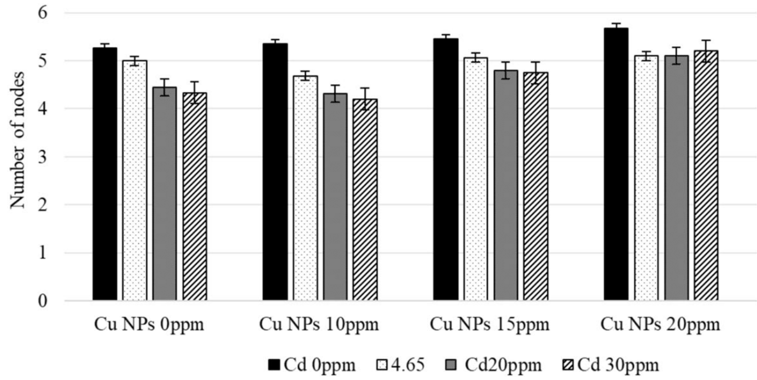

Fig. 10. Impact of different concentrations of Cd and MA- CuO NPs on the number of nodes of *T. aestivum*.

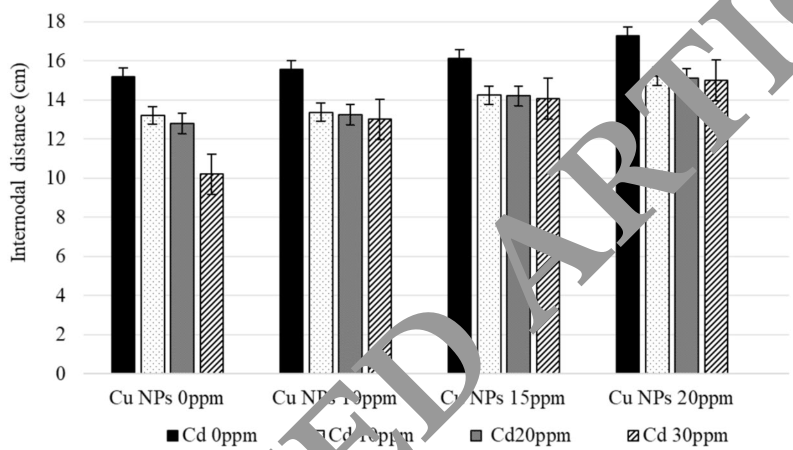

Fig. 11. Impact of different concentrations of Cd and MA- CuO NPs on the internodal distance of *T. aestivum*.

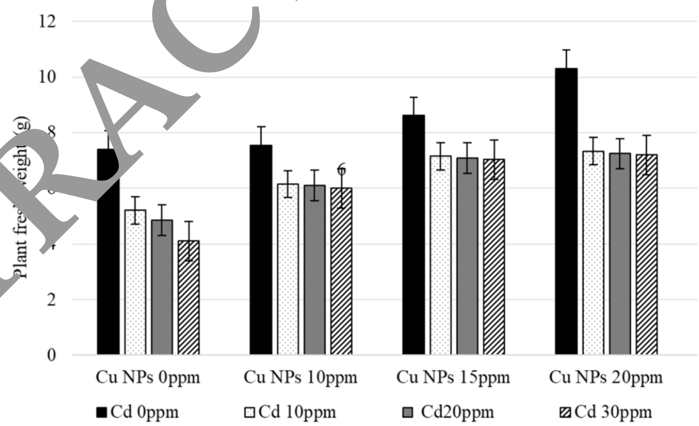

Fig. 12. Impact of different concentrations of Cd and MA- CuO NPs on the total plant fresh weight of *T. aestivum*.

CuONP), the total plant fresh weight was 7.40 g. Under severe Cd stress (30 ppm, 0 ppm MA-CuONP), the fresh weight decreased to 4.10 g, representing a 44.4% reduction compared with that of the control, highlighting the detrimental impact of Cd. Conversely, with 20 ppm MA-CuONPs and no Cd stress, the fresh weight increased to 10.30 g, indicating a 39.0% increase from that of the control. The combination of 10 ppm MA-CuO NPs with 30 ppm Cd resulted in a fresh weight of 6.00 g, reflecting an 18.9% increase compared with that of the control. The application of 15 ppm MA-CuONPs in conjunction with 30 ppm Cd resulted in a fresh weight of 7.03 g, which was 0.4% greater than that of the control (Fig. 12).

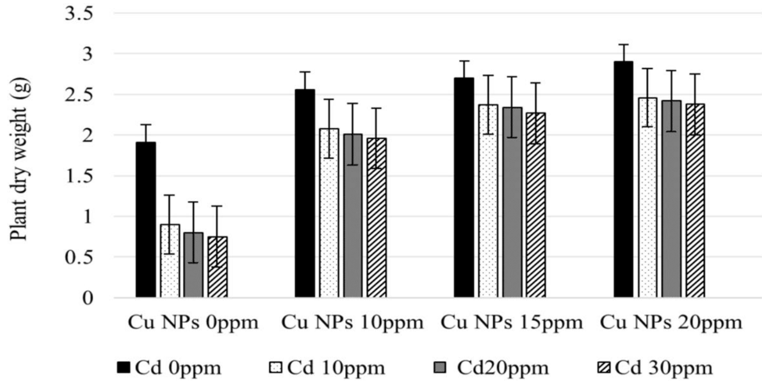

Fig. 13. Impact of different concentrations of Cd and MA- CuO NPs on the total plant dry weight of *T. aestivum*.

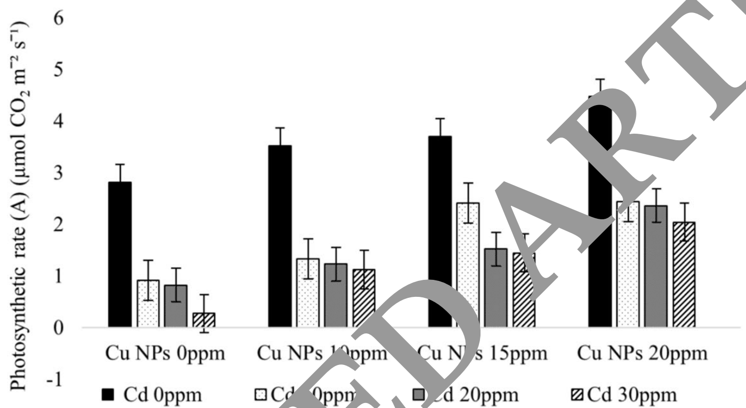

Fig. 14. Impact of different concentrations of Cd and MA-CuO NPs on the photosynthetic rate of *T. aestivum*.

The total dry weight of *T. aestivum* plants grown with different concentrations of Cd and MA-CuONPs was also determined. Under the control conditions (0 ppm Cd, 0 ppm MA-CuONP), the total dry weight was 1.91 g. Under severe Cd stress (30 ppm, 0 ppm MA-CuONP), the dry weight decreased to 0.75 g, representing a 60.8% reduction compared with that of the control, highlighting the detrimental impact of Cd. Conversely, with 20 ppm MA-CuONPs and no Cd stress, the dry weight increased to 2.90 g, indicating a 51.9% increase from that of the control. The combination of 10 ppm MA-CuONPs with 30 ppm Cd resulted in a dry weight of 1.96 g, reflecting a 2.1% increase compared with that of the control. The application of 15 ppm MA-CuONPs in conjunction with 30 ppm Cd resulted in a dry weight of 2.27 g, which was 19.0% greater than that of the control. These results suggest that while Cd stress significantly reduces dry weight, the application of MA-CuONPs can alleviate this effect and increase growth, especially at relatively high concentrations (Fig. 13).

Effects of different concentrations of Cd and MA-CuO NPs on the photosynthetic rate, transpiration rate, stomatal conductance and intracellular CO_2 concentration

The photosynthetic rates of *T. aestivum* under various concentrations of cadmium and MA-CuO were significantly different among the treatment means. Under control conditions (0 ppm Cd, 0 ppm MA-CuO NPs), the photosynthetic rate was 2.81 μmol CO_2 m^{-2} s^{-1}. Under severe Cd stress (30 ppm, MA-CuO NPs 0 ppm), it decreased to 0.272 μmol CO_2 m^{-2} s^{-1}, representing a 90.3% reduction. In contrast, with 20 ppm MA-CuO NPs and no Cd stress, the rate increased to 4.47 μmol CO_2 m^{-2} s^{-1}, a 59.1% increase compared with that of the control. The combination of 10 ppm MA-CuO NPs with 30 ppm Cd resulted in a rate of 1.12 μmol CO_2 m^{-2} s^{-1}, reflecting a 60.1% reduction, whereas 15 ppm MA-CuO NPs with 30 ppm Cd improved the rate to 1.44 μmol CO_2 m^{-2} s^{-1}, showing a 48.8% reduction. These findings indicate that Cd stress significantly impairs photosynthetic performance, but MA-CuO NPs, particularly at relatively high concentrations, can help mitigate this effect (Fig. 14). Under control conditions (0 ppm Cd, 0 ppm MA-CuO NPs), the transpiration rate was 1.32 mmol H_2O m^{-2} s^{-1}. Under severe Cd stress (30 ppm, 0 ppm MA-CuO NPs), the transpiration rate decreased to 0.44 mmol H_2O m^{-2} s^{-1}, representing a 66.7% reduction compared with that of the control. With 20 ppm MA-CuO NPs and no Cd stress, the transpiration rate increased to 1.66 mmol H_2O m^{-2} s^{-1}, indicating a 25.8% increase compared with that of the control. The combination of 10 ppm MA-CuO NPs with 30 ppm Cd resulted in a transpiration rate of 0.78 mmol H_2O m^{-2} s^{-1}, reflecting a 40.9% reduction compared with that of the

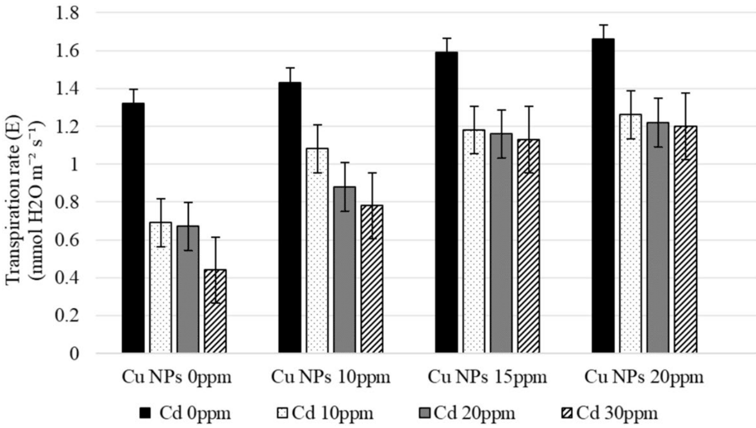

Fig. 15. Impact of different concentrations of Cd and MA- CuO NPs on the transpiration rate of *T. aestivum*.

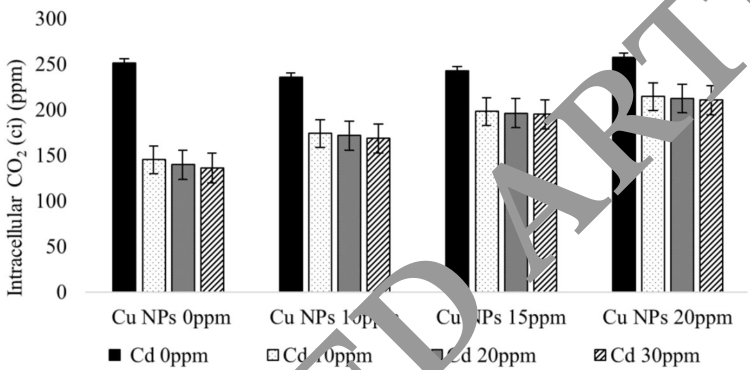

Fig. 16. Impact of different concentrations of Cd and MA-CuO NPs on the stomatal conductance of *T. aestivum*.

control. Similarly, applying 15 ppm MA-CuO NPs under 30 ppm Cd stress increased the transpiration rate to 1.13 mmol H_2O m^{-2} s^{-1}, a 14.4% reduction relative to that of the control (Fig. 15). The stomatal conductance of *T. aestivum* under varying concentrations of Cd and MA-CuO NPs also significantly differed among the treatment methods. Under control conditions (0 ppm Cd, 0 ppm MA-CuO NPs), the stomatal conductance was 2.27 mmol H_2O m^{-2} s^{-1}. Under severe Cd stress (30 ppm, MA-CuO NPs 0 ppm), it decreased to 0.55 mmol H_2O m^{-2} s^{-1}, representing a 75.8% reduction compared with that of the control. With 20 ppm MA-CuO NPs and no Cd stress, the stomatal conductance increased to 2.61 mmol H_2O m^{-2} s^{-1}, showing a 15% improvement compared with that of the control. The combination of 10 ppm MA-CuO NPs with 30 ppm Cd resulted in a stomatal conductance of 1.13 mmol H_2O m^{-2} s^{-1}, reflecting a 50.2% reduction compared with that of the control. Similarly, applying 15 ppm MA-CuO NPs under 30 ppm Cd stress increased the stomatal conductance to 1.25 mmol H_2O m^{-2} s^{-1}, representing a 45% reduction compared with that of the control (Fig. 16). Under control conditions (0 ppm Cd, 0 ppm MA-CuO NPs), the intracellular CO_2 concentration was 251.37 ppm. Under severe Cd stress (30 ppm, MA-CuO NPs 0 ppm), it decreased to 136.07 ppm, representing a 45.9% reduction compared with that of the control. With 20 ppm MA-CuO NPs and no Cd stress, the intracellular CO_2 concentration increased to 257.39 ppm, indicating a 2.4% improvement over the control. The combination of 10 ppm MA-CuO NPs with 30 ppm Cd resulted in an intracellular CO_2 concentration of 168.19 ppm, reflecting a 33.1% reduction compared with that of the control. Similarly, the application of 15 ppm MA-CuO NPs under 30 ppm Cd stress increased the concentration to 194.64 ppm, a 22.6% reduction relative to that of the control (Fig. 17).

Effects of different concentrations of Cd and MA-CuO NPs on CO_2 drop, water use efficiency and relative water content

The CO_2 drop of *T. aestivum* under varying concentrations of Cd and MA-CuO NPs is described. Under control conditions (0 ppm Cd, 0 ppm MA-CuO NPs), the CO_2 drop was 35.66 ppm. Under severe Cd stress (30 ppm, MA-CuO NPs 0 ppm), it decreased to 9.2 ppm, representing a 74.2% reduction compared with that of the control. With 20 ppm MA-CuO NPs and no Cd stress, the CO_2 decrease increased to 65.63 ppm, indicating an 84% improvement over the control. The combination of 10 ppm MA-CuO NPs with 30 ppm Cd resulted in a decrease in CO_2 to 17.6 ppm, reflecting a 50.6% reduction compared with that of the control. Similarly, applying

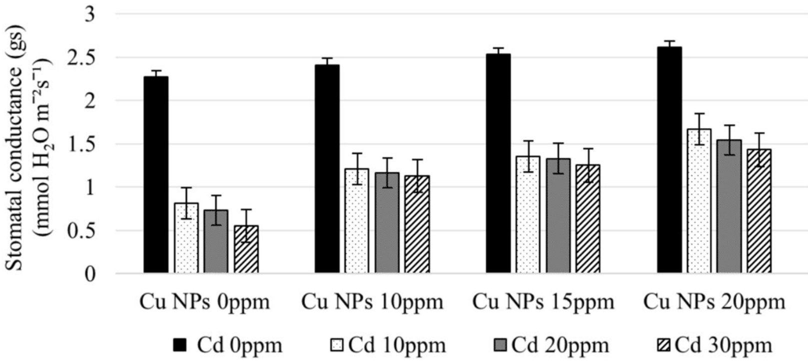

Fig. 17. Impact of different concentrations of Cd MA- CuO NPs on the intracellular CO_2 of *T. aestivum*.

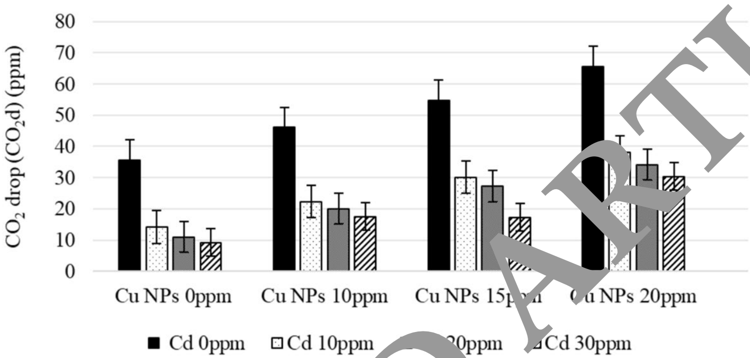

Fig. 18. Impact of different concentrations of Cd and MA-CuO NPs on the CO_2 drop of *T. aestivum*.

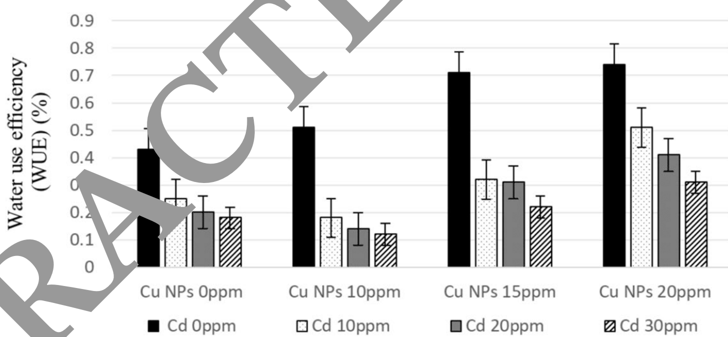

Fig. 19. Impact of different concentrations of Cd and MA-CuO NPs on the water use efficiency of *T. aestivum*.

15 ppm MA-CuO NPs under 30 ppm Cd stress caused the CO_2 concentration to decrease to 17.4 ppm, a 51.2% reduction relative to that of the control (Fig. 18).

Under control conditions (0 ppm Cd, 0 ppm MA-CuO NPs), the water use efficiency was 0.43. Under severe Cd stress (30 ppm, MA-CuO NPs 0 ppm), the value decreased to 0.18, representing a 58.1% reduction compared with that of the control. With 20 ppm MA-CuO NPs and no Cd stress, the water use efficiency improved to 0.74, indicating a 72.1% increase compared with that of the control. The combination of 10 ppm MA-CuO NPs with 30 ppm Cd resulted in a water use efficiency of 0.12, reflecting a 72.1% reduction compared with that of the control. Similarly, applying 15 ppm MA-CuO NPs under 30 ppm Cd stress increased the efficiency to 0.22, a 48.8% reduction relative to that of the control (Fig. 19). The relative water content (RWC) of *T. aestivum* under different concentrations of Cd and MA-CuO NPs also significantly differed among the treatment methods. Under control conditions (0 ppm Cd, 0 ppm MA-CuO NPs), the RWC was 0.82. Under severe Cd stress (30 ppm, MA-CuO NPs 0 ppm), it decreased to 0.59, representing a 28.0% reduction compared with that of the control. With 20 ppm MA-CuO NPs and no Cd stress, the RWC increased to 1.20, indicating a 46.3% improvement compared with that of the control. The combination of 10 ppm MA-CuO NPs with 30 ppm Cd resulted in an RWC of 0.81,

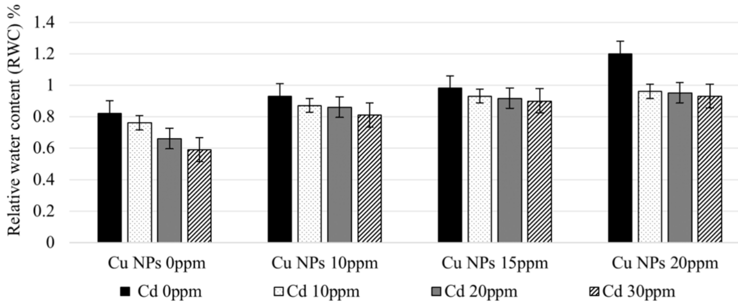

Fig. 20. Impact of different concentrations of Cd and MA-CuO NPs on the relative water content of *T. aestivum*.

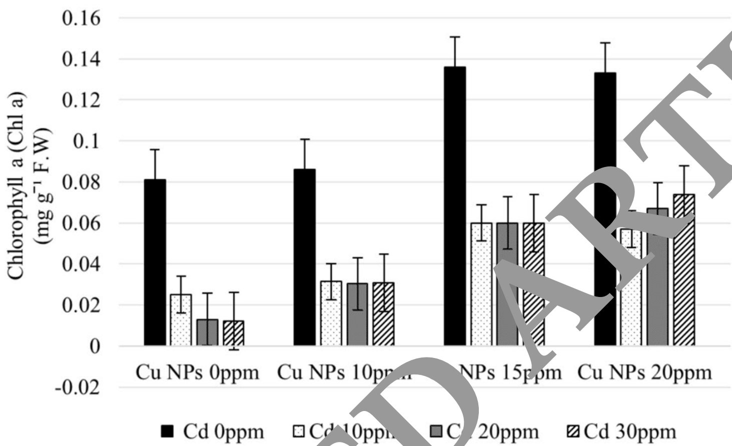

Fig. 21. Impact of different concentrations of Cd and MA-CuO NPs on the Chl a of *T. aestivum*.

reflecting a 1.2% reduction compared with that of the control. Similarly, applying 15 ppm MA-CuO NPs under 30 ppm Cd stress caused the RWC to decrease to 0.90, a 9.8% reduction relative to that of the control (Fig. 20).

Effects of different concentrations of Cd and MA-CuO NPs on chla, chlb, carotenoids and total chlorophyll

The chlorophyll a (Chl a) content of *T. aestivum* under different concentrations of Cd and MA-CuO NPs was significantly different among the treatment means. Under control conditions (0 ppm Cd, 0 ppm MA-CuO NPs), the Chl a content was 0.081 mg g^{-1}. Under severe Cd stress (30 ppm, MA-CuO NPs 0 ppm), the content decreased to 0.012 mg g^{-1}, representing an 85.2% reduction compared with that of the control. With 20 ppm MA-CuO NPs and no Cd stress, the Chl a content increased to 0.133 mg g^{-1}, indicating a 64.2% improvement over the control. The combination of 10 ppm MA-CuO NPs with 30 ppm Cd resulted in a Chl a content of 0.0307 mg g^{-1}, reflecting a 62.0% reduction compared with that of the control. Similarly, the application of 15 ppm MA-CuO NPs under 30 ppm Cd stress caused the Chl a content to remain at 0.06 mg g^{-1}, which was a 26.9% reduction relative to that of the control (Fig. 21). Under control conditions (0 ppm Cd, 0 ppm MA-CuO NPs), the Chl b content was 2.51 mg g^{-1}. Under severe Cd stress (30 ppm, 0 ppm MA-CuO NPs), the content decreased to 0.61 mg g^{-1}, representing a 75.7% reduction compared with that of the control. With 20 ppm MA-CuO NPs and no Cd stress, the Chl b content increased to 4.32 mg g^{-1}, indicating a 72.0% improvement over the control. The combination of 10 ppm MA-CuO NPs with 30 ppm Cd resulted in a Chl b content of 2.76 mg g^{-1}, reflecting a 9.4% reduction compared with that of the control. Similarly, the application of 15 ppm MA-CuO NPs under 30 ppm Cd stress caused the Chl b content to decrease to 3.17 mg g^{-1}, a 26.3% reduction relative to that of the control (Fig. 22). The carotenoid contents of *T. aestivum* under different concentrations of Cd and MA-CuO NPs are also discussed. Under control conditions (0 ppm Cd, 0 ppm MA-CuO NPs), the carotenoid content was 1.08 mg g^{-1}. Under severe Cd stress (30 ppm, MA-CuO NPs 0 ppm), the content decreased to 0.60 mg g^{-1}, representing a 44.4% reduction compared with that of the control. With 20 ppm MA-CuO NPs and no Cd stress, the carotenoid content increased to 2.10 mg g^{-1}, indicating a 94.4% improvement over the control. The combination of 10 ppm MA-CuO NPs with 30 ppm Cd resulted in a carotenoid content of 1.12 mg g^{-1}, reflecting a 3.7% reduction compared with that of the control. Similarly, the application of 15 ppm MA-CuO NPs under 30 ppm Cd stress caused the carotenoid content to decrease to 1.54 mg g^{-1}, a 16.9% reduction relative to that of the control (Fig. 23). The total chlorophyll content of *T. aestivum* under varying concentrations of Cd and MA-CuO NPs is presented. Under control conditions (0 ppm Cd, 0 ppm MA-CuO NPs), the total chlorophyll

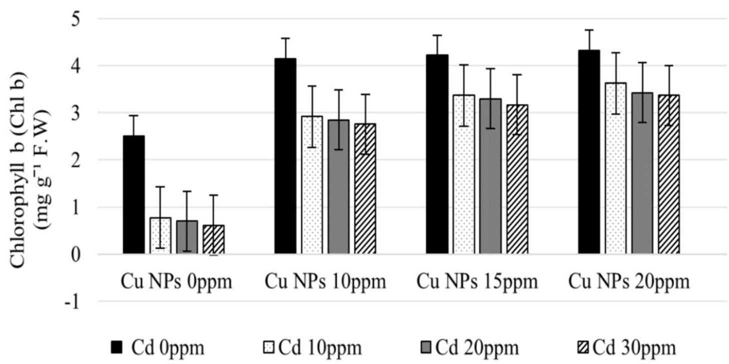

Fig. 22. Impact of different concentrations of Cd and MA-CuO NPs on the Chl b of *T. aestivum*.

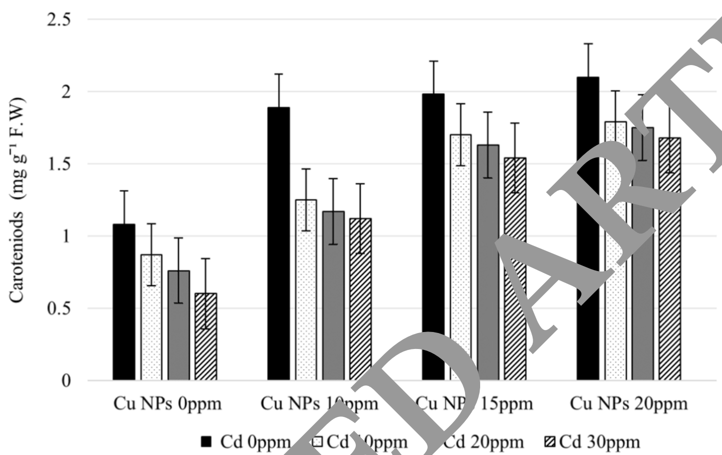

Fig. 23. Impact of different concentrations of Cd and MA-CuO NPs on the carotenoids of *T. aestivum*.

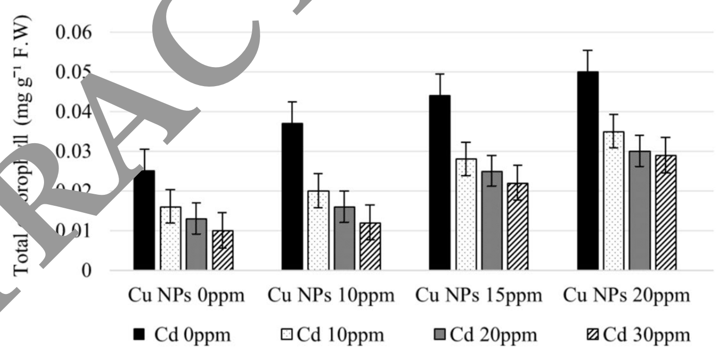

Fig. 24. Impact of different concentrations of Cd and MA-CuO NPs on the total chlorophyll content of *T. aestivum*.

content was 0.025 mg g^{-1}. Under severe Cd stress (30 ppm, 0 ppm MA-CuO NPs), the content decreased to 0.010 mg g^{-1}, representing a 60.0% reduction compared with that of the control. With 20 ppm MA-CuO NPs and no Cd stress, the total chlorophyll content increased to 0.050 mg g^{-1}, indicating a 100% improvement over the control. Compared with the control, the combination of 10 ppm MA-CuO NPs with 30 ppm Cd resulted in a total chlorophyll content of 0.012 mg g^{-1}, reflecting a 52.0% reduction. Similarly, applying 15 ppm MA-CuO NPs under 30 ppm Cd stress caused the total chlorophyll content to decrease to 0.022 mg g^{-1}, a 12.0% reduction relative to that of the control (Fig. 24).

Effects of different concentrations of Cd and MA-CuO NPs on stem length, width and surface area

The stem length of *T. aestivum* under varying concentrations of Cd and MA-CuO NPs significantly differed among the treatment methods. Under control conditions (0 ppm Cd, 0 ppm MA-CuO NPs), the stem length was 6.15 cm. Under severe Cd stress (30 ppm), it decreased to 4.52 cm, representing a 26.5% reduction compared with that of the control (Table 1). The application of 10 ppm MA-CuO NPs improved the stem length to 5.0 cm, indicating an 18.7% reduction under the same Cd concentration. With 15 ppm MA-CuO NPs, the stem length was 5.89 cm, reflecting a 4.3% reduction compared with that of the control. Interestingly, 20 ppm MA-CuO NPs maintained a stem length of 5.98 cm, indicating a 2.8% reduction compared with that of the control (Fig. 25). The stem width in the control treatment was 5.84 cm, which decreased to 4.53 cm under severe Cd stress, representing a 22.4% reduction. The application of 10 ppm MA-CuO NPs resulted in a stem width of 4.27 cm under 30 ppm Cd stress that indicating a 26.8% reduction. With 15 ppm MA-CuO NPs, the stem width was 5.13 cm, showing a 12.0% reduction compared with that of the control. The use of 20 ppm MA-CuO NPs led to a stem width of 5.30 cm, reflecting a 9.2% reduction compared with that of the control (Fig. 26). For the stem surface area, the control condition was 28.01 cm^2. Under severe Cd stress (30 ppm), it decreased to 20.58 cm^2 and representing a 26.5% reduction compared with that of the control. The application of 10 ppm MA-CuO NPs increased the stem surface area to 21.35 cm^2, indicating a 23.7% reduction. With 15 ppm MA-CuO NPs, the surface area increased to 30.24 cm^2, reflecting a 7.8% reduction compared with that of the control. Finally, 20 ppm MA-CuO NPs resulted in a stem surface area of 31.69 cm^2, which was 13.8% improvement over that of the control (Fig. 27).

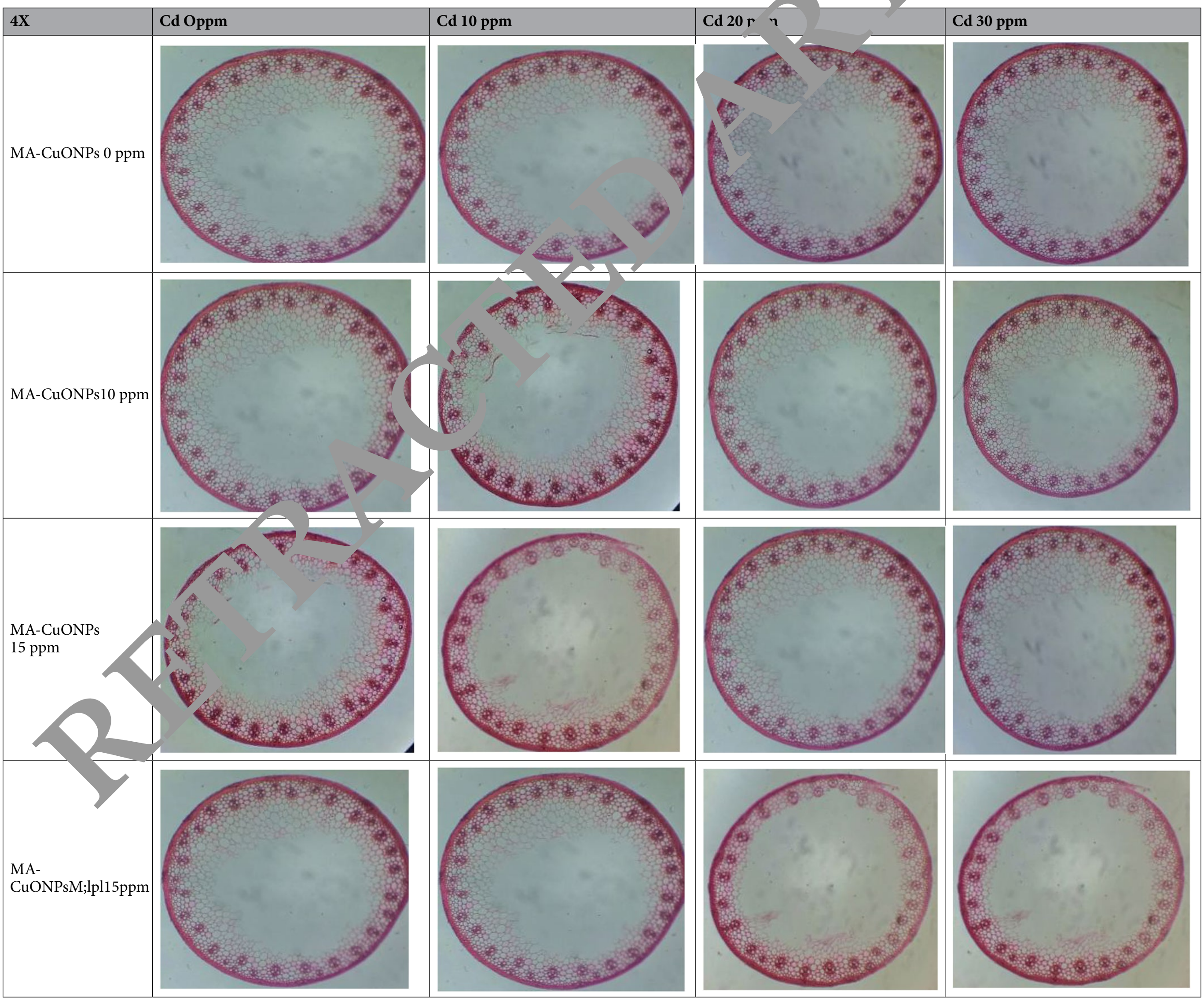

Table 1. Effects of different concentrations of Cd and MA-CuO NPs on stem length, width and surface area.

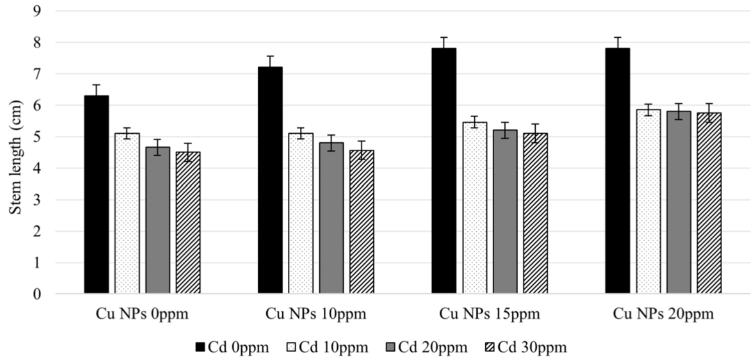

Fig. 25. Impact of different concentrations of cadmium and MA-CuO-based NPs on the stem length of *T. aestivum*.

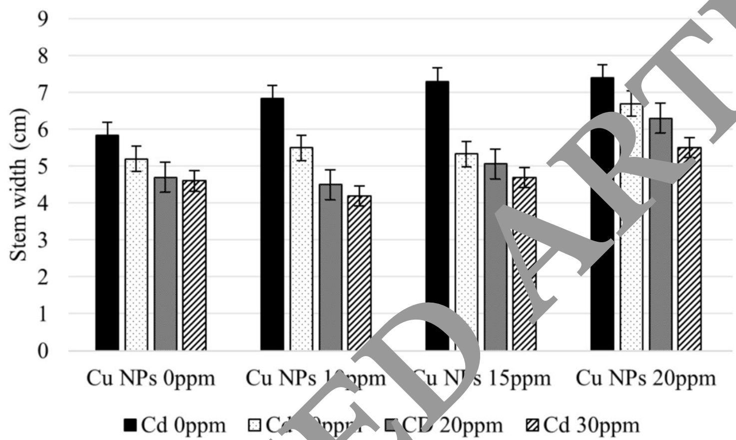

Fig. 26. Impact of different concentrations of cadmium and MA-CuO-based NPs on the stem width of *T. aestivum*.

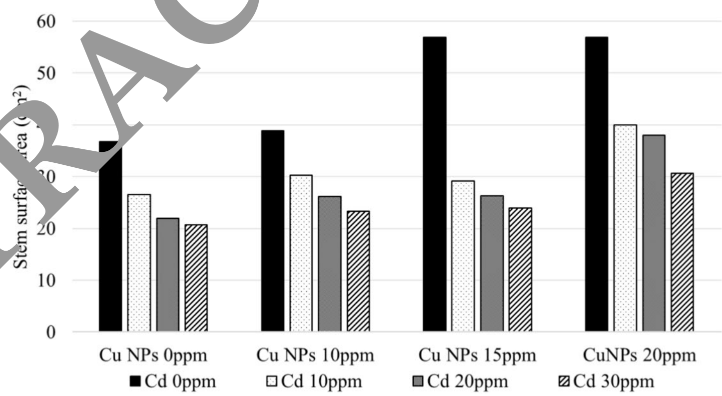

Fig. 27. Impact of different concentrations of cadmium and MA-CuO-based NPs on the stem surface area of *T. aestivum*.

Effects of different concentrations of Cd and MA-CuO NPs on root length, width and surface area

The root length of *T. aestivum* under varying concentrations of Cd and MA-CuO NPs significantly differed among the treatment means (Table 2). Under control conditions (0 ppm Cd, 0 ppm MA-CuONP), the root length was 6.15 cm. Compared with that of the control, the depth under 30 ppm Cd stress decreased to 4.75 cm, representing a 22.8% reduction. The application of 10 ppm MA-CuONPs improved the root length to 5.3 cm (13.8% reduction), and 20 ppm MA-CuO NPs maintained a length of 6.1 cm (0.8% reduction) at the same Cd

4X	Cd Oppm	Cd 10 ppm	Cd 20 ppm	Cd 30 ppm
MACuONPs 0 ppm	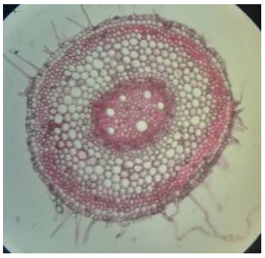	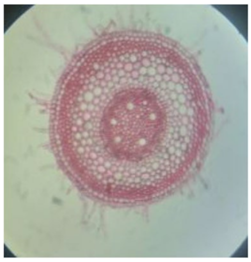	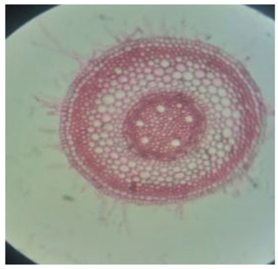	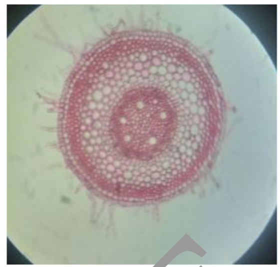
MA-CuONPs 10 ppm	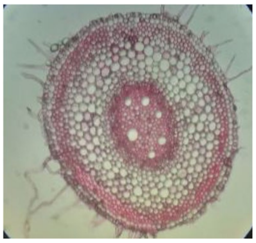	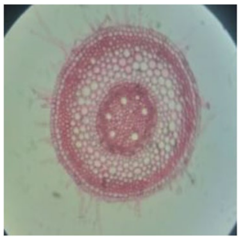	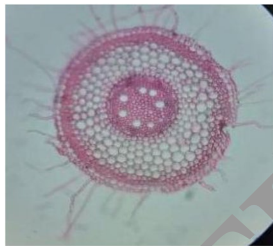	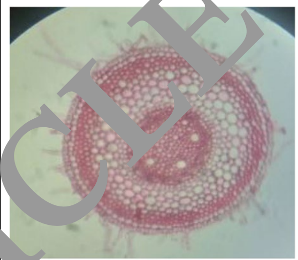
MA-CuONPs 15 ppm	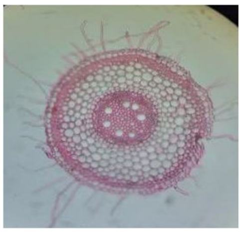	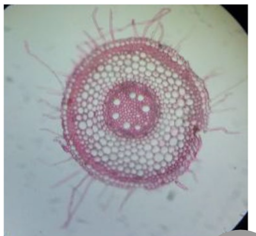		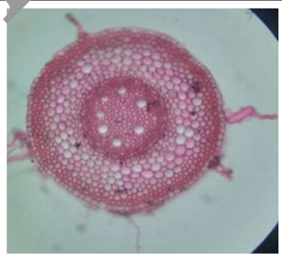
MA-CuONPs 20 ppm	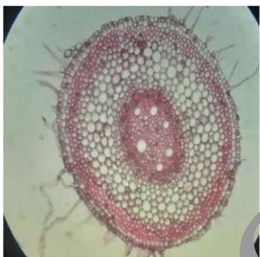	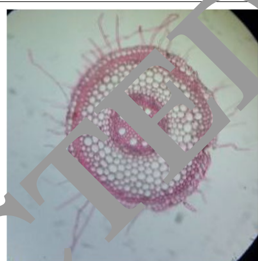	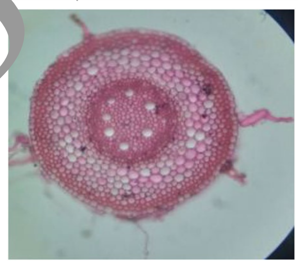	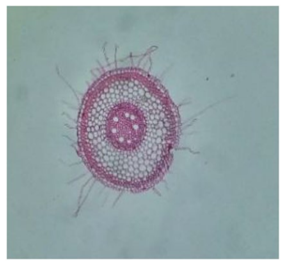

Table 2. Effects of different concentrations of Cd and MA-CuO NPs on root length, width and surface area.

concentration (Fig. 28). The width of the roots in the control treatment was 5.66 mm, which decreased to 4.2 cm under severe Cd stress (25.7% reduction). With 10 ppm MA-CuO NPs, the root width was 4.88 cm (13.8% reduction) under 30 ppm Cd stress (Fig. 29). The root surface area initially recorded at 34.83 cm^2 under control conditions decreased to 19.95 cm^2 (42.6% reduction) at 30 ppm Cd. The application of 10 ppm MA-CuONPs improved the surface area to 24.61 cm^2 (29.4% reduction), whereas 15 ppm MA-CuONPs yielded 27.25 cm^2 (21.9% reduction), and 20 ppm MA-CuONPs reached 36.06 cm^2 (17.1% reduction), highlighting the protective effects of the nanoparticles against Cd toxicity (Fig. 30).

Effects of different concentrations of Cd and MA-CuO NPs on spike length, number of spikelets and number of grains

The spike length of *T. aestivum* under varying concentrations of Cd and MA-CuO NPs significantly differed among the treatment means. Under control conditions (0 ppm Cd, 0 ppm MA-CuO NPs), the spike length was 11.02 cm. Under severe Cd stress (30 ppm), it decreased to 8.37 cm, representing a 24.1% reduction compared with that of the control. Compared with the control, the application of 10 ppm MA-CuO NPs improved the spike length to 12.79 cm, indicating a 7.1% reduction. With 15 ppm MA-CuO NPs, the spike length remained at 13.03 cm, indicating a 3.9% reduction under the same Cd concentration. Interestingly, 20 ppm MA-CuO NPs maintained a spike length of 13.12 cm, reflecting a 1.9% reduction compared with that of the control (Fig. 31).

In terms of the number of spikelets, the control condition resulted in 12.94 spikelets. Under 30 ppm Cd stress, it decreased to 12.16%, representing a 5.9% reduction compared with that of the control. Compared with the control, the application of 10 ppm MA-CuO NPs increased the number of spikelets to 12.06, indicating a 6.8% reduction. With 15 ppm MA-CuO NPs, the number of spikelets increased to 13.14, showing a 1.8% reduction under the same Cd concentration. The use of 20 ppm MA-CuO NPs led to 14.33 spikelets, reflecting a 10.6% improvement compared with the control (Fig. 32).

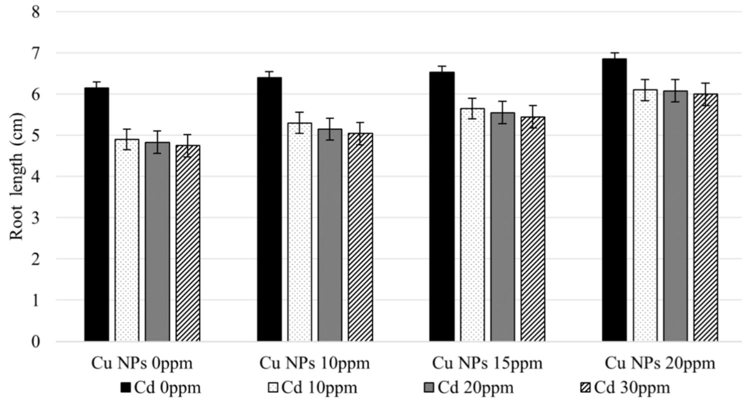

Fig. 28. Impact of different concentrations of cadmium and MA-CuO-based NPs on the root length of *T. aestivum*.

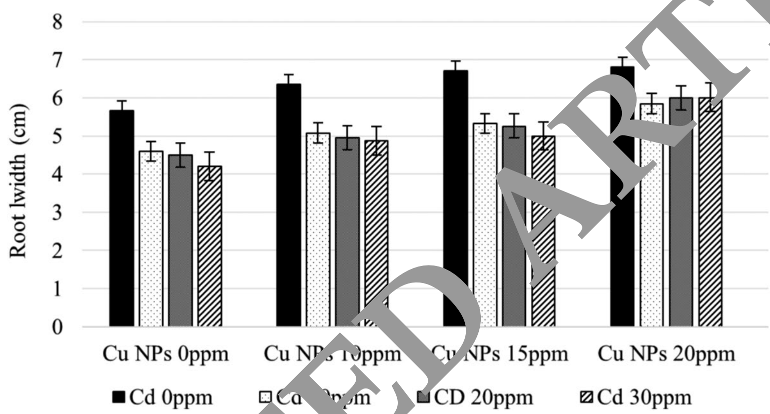

Fig. 29. Impact of different concentrations of cadmium and MA-CuO-based NPs on the stem width of *T. aestivum.*

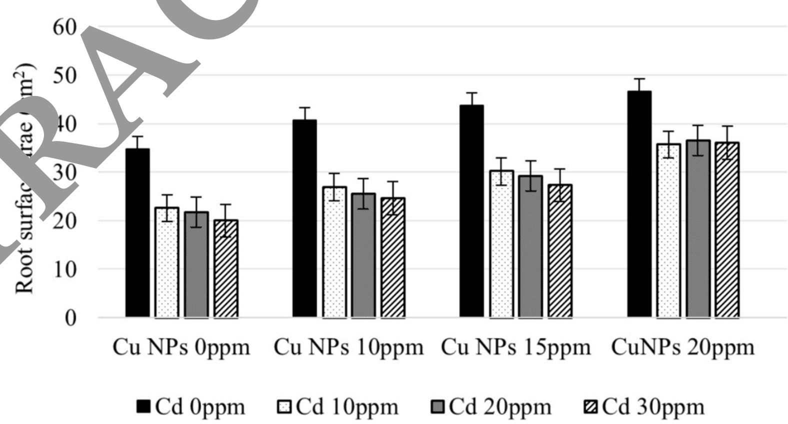

Fig. 30. Impact of different concentrations of cadmium and MA-CuO-based NPs on the stem surface area of *T. aestivum*.

For the number of grains, the control condition resulted in 38.67 grains. Under severe Cd stress (30 ppm), it decreased to 32 grains, representing a 17.4% reduction compared with that of the control. The application of 10 ppm MA-CuO NPs increased the number of grains to 36.33, indicating a 6.0% reduction. With 15 ppm MA-CuO NPs, the number of grains rose to 39.45, reflecting a 2.8% reduction compared with that of the control. Finally, 20 ppm MA-CuO NPs resulted in 42.33 grains, showing a 9.6% improvement over the control (Fig. 33).

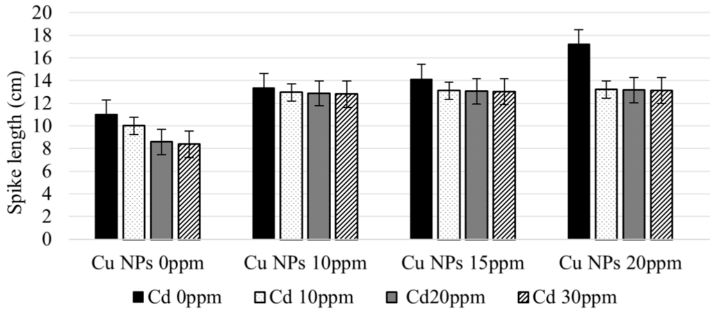

Fig. 31. Impact of different concentrations of cadmium and MA-CuO-based NPs on the spike length of *T. aestivum*.

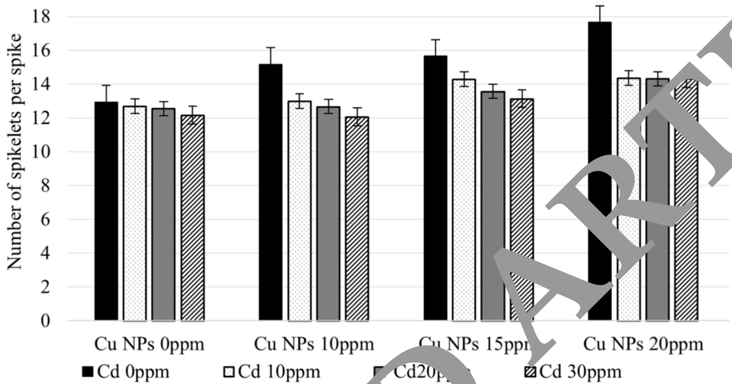

Fig. 32. Impact of different concentrations of cadmium and MA-CuO-based NPs on the number of spikelets of *T. aestivum*.

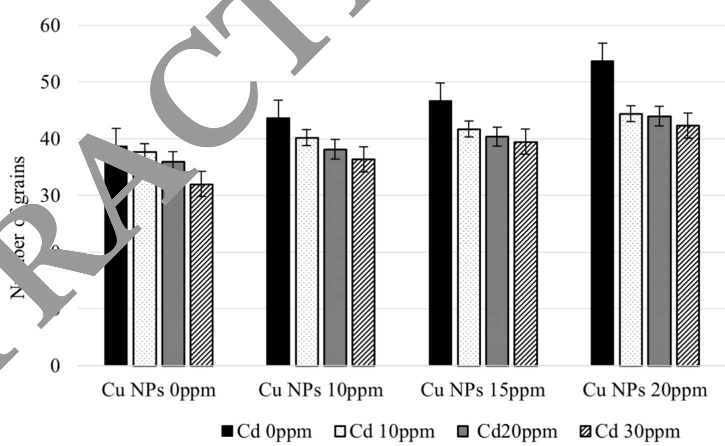

Fig. 33. Impact of different concentrations of cadmium and MA-CuO-based NPs on the number of grains of *T. aestivum*.

Effects of different concentrations of Cd and MA-CuO NPs on spike fresh and dry weights

The spike fresh weights of *T. aestivum* under various concentrations of Cd and MA-CuO NPs were significantly different among the treatment means. Under the control conditions (0 ppm Cd, 0 ppm MA-CuO NPs), the spike fresh weight was 2.6 g. Under severe Cd stress (30 ppm, 0 ppm MA-CuO NPs), it decreased to 2.05 g, representing a 21.2% reduction compared with that of the control, highlighting the adverse effects of Cd stress.

With 20 ppm MA-CuO NPs and no Cd stress, the spike fresh weight increased to 2.78 g, which was a 6.9% improvement over that of the control. The combination of 10 ppm MA-CuO NPs with 30 ppm Cd resulted in a spike fresh weight of 2.33 g, reflecting a 10.4% reduction compared with that of the control. Similarly, applying 15 ppm MA-CuO NPs under 30 ppm Cd stress resulted in a spike fresh weight of 2.47 g, a 7.1% reduction relative

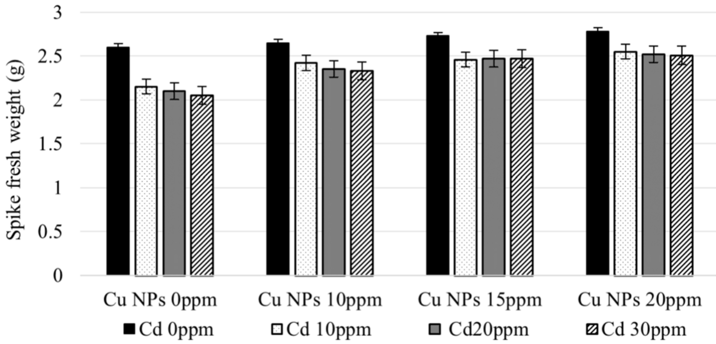

Fig. 34. Impact of different concentrations of cadmium- and MA-CuO-based NPs on the spike fresh weight of *T. aestivum*.

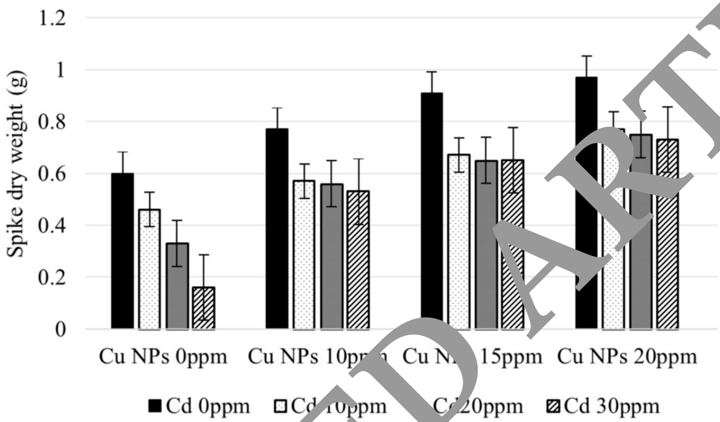

Fig. 35. Impact of different concentrations of cadmium- and MA-CuO-based NPs on the spike dry weight of *T. aestivum*.

to that of the control. At 20 ppm MA-CuO NPs with 30 ppm Cd stress, the spike fresh weight reached 2.51 g, showing only a [illegible]5% reduction compared with that of the control, indicating improved resilience at higher nanoparticle concentrations (Fig. 34). Under the control conditions (0 ppm Cd, 0 ppm MA-CuO NPs), the spike dry weight was 0.6 g. Under severe Cd stress (30 ppm, 0 ppm MA-CuO NPs), the spike dry weight decreased to 0.16 g, representing a significant 73.3% reduction compared with that of the control, demonstrating the detrimental effect of Cd stress. With 20 ppm MA-CuO NPs and no Cd stress, the spike dry weight increased to 0.97 g, reflecting a 61.7% improvement over the control. Compared with the control, the combination of 10 ppm MA-CuO NPs with 30 ppm Cd resulted in a spike dry weight of 0.53 g, which was an 11.7% reduction. Similarly, applying 15 ppm MA-CuO NPs under 30 ppm Cd stress resulted in a spike dry weight of 0.65 g, reflecting an 8.3% increase compared with that of the control. At 20 ppm MA-CuO NPs with 30 ppm Cd stress, the spike dry weight reached 0.73 g, indicating a 21.7% improvement relative to that of the control, demonstrating the effectiveness of higher nanoparticle concentrations in alleviating Cd stress (Fig. 35).

Discussion

Green-synthesized copper oxide nanoparticles (CuO NPs) effectively mitigate cadmium (Cd) stress in wheat (*Triticum aestivum* L.) by enhancing plant growth and physiological resilience[14,15]. The results of this study show that CuO NPs reduce Cd uptake and increase antioxidant defenses, indicating their potential as a viable strategy to counteract heavy metal toxicity in crops. These findings offer valuable insights into using nanoparticles as sustainable interventions for improving crop performance in contaminated soils. The goal of the current study was to determine how MA-CuONPs could help *T. aestivum,* particularly the Arooj-22 type, reduce the effects of Cd stress. This study investigated the effects of different Cd concentrations (0, 10, 20, and 30 ppm) on plant growth and development, as well as the ways in which different MA-CuONP concentrations (0, 10, 15, and 20 ppm) mitigate these effects. The results of this study demonstrated that Cd stress significantly impaired the growth and biomass accumulation of *T. aestivum.* Compared with those under the control, the plant height, shoot height, and root length under 30 ppm Cd stress decreased by 25.6%, 19.5%, and 34.1%, respectively, whereas the fresh and dry weights were reduced by 44.4% and 60.8%, respectively. The findings of this study align with those of Aslam et al.[37], reported that Cd stress negatively impacted various growth parameters, including plant height

(35.9 cm) and root and shoot lengths (16.2 cm and 19.8 cm), and reduced the fresh and dry weights of shoots (13.6 g and 0.87 g) and roots (1.82 g and 0.08 g).

However, the application of MA-CuO NPs effectively increased the growth parameters. In the absence of Cd, 20 ppm MA-CuO NPs increased plant height, shoot height, and root length by 53%, 85.1%, and 32.1%, respectively, compared with those of the control. Notably, even under 30 ppm Cd stress, applying 10 and 15 ppm MA-CuO NPs improved shoot height by 4.2% and 30.4%, respectively, and root length by 17.1% and 10.3%, underscoring the mitigating role of MA-CuO NPs against Cd-induced stress. The application of 20 ppm MA-CuO NPs significantly improved the growth parameters of *T. aestivum* under nonstress conditions[38]. Compared to the control, plant height increased by 53% (reaching 92 cm), shoot height by 85.1% (92.4 cm), and root length by 32.1% (4.81 cm). Similarly, the number of leaves increased by 35.7% (7.68), the number of nodes increased by 7.9% (5.68), and the internodal distance increased by 13.4% (17.26 cm). These results suggest that MA-CuO NPs enhance plant growth, indicating their potential for promoting biomass accumulation and vegetative development[39,40].

The results of this study are in accordance with recent investigations into the effects of copper nanoparticles (CuNPs) on the growth of wheat. Raza et al.[41] explored the influence of CuNPs on wheat health and reported that concentrations ranging from 25 to 50 mg L^{-1} significantly increased various growth metrics, including plant height and biomass accumulation. However, studies addressing additional parameters such as the number of leaves, number of nodes, and internodal distance are lacking. In contrast, this research comprehensively examined these aspects, revealing that CuNPs also positively influence these growth traits, providing a more holistic understanding of their effects on wheat development[42].

This study revealed that cadmium (Cd) stress has a pronounced negative effect on the photosynthetic performance of *T. aestivum*. Specifically, under severe Cd stress at 30 ppm, the photosynthetic rate plummeted by 90.3%, whereas the transpiration rate decreased by 66.7%. The stomatal conductance also significantly decreased by 75.8%, and the intracellular CO_2 concentration was 45.9% lower than that in the control. Conversely, the application of 20 ppm MA-CuO NPs led to a notable increase of 59.1% in the photosynthetic rate and an impressive 84% improvement in the CO_2 decrease relative to those of the control group. Ahmed et al.[43] reported that when plants were spiked with Cd, the greatest reductions in the transpiration rate, stomatal conductance, and photosynthetic rate (59.67%, 47.63%, and 59.15%, respectively) were detected.

However, there is a notable lack of research addressing the specific parameters of CO_2 drop, water use efficiency, and relative humidity. This research comprehensively examined these critical physiological aspects, revealing how Cd stress impacts *T. aestivum*. By investigating these parameters, this study provides a more in-depth understanding of how Cd concentrations influence plant performance, highlighting the essential role of MA-CuO NPs in mitigating these adverse effects[44]. Compared with the control, the application of 20 ppm MA-CuO nanoparticles significantly increased the physiological parameters of *T. aestivum*, resulting in a 59.1% increase in the photosynthetic rate, a 25.8% improvement in the transpiration rate, and an 84% increase in the decrease in CO_2. Additionally, the water use efficiency improved by 72.1%, indicating the potential of Cu NPs to promote plant growth and resilience. However, it is important to note that there is currently no literature that specifically investigates the impact of MA-CuO nanoparticles on the IRGA parameters in wheat plants, making this study a pioneering contribution to the field[45]. This study revealed that Cd stress negatively affects the chlorophyll and carotenoid contents of *T. aestivum*. Specifically, compared with the control, 30 ppm Cd reduced chlorophyll a by 85.2%, chlorophyll b by 75.7%, and carotenoids by 44.4%. In contrast, the application of 20 ppm MA-CuO NPs significantly improved the contents of photosynthetic pigments. The content of chlorophyll an increased by 64.2%, that of chlorophyll b increased by 72.0%, and that of carotenoids increased by 94.4%. When combined with Cd stress, 10 ppm MA-CuO NPs reduced the impact, although chlorophyll a and b decreased by 62.0% and 9.[illegible]%, respectively, while carotenoids decreased by 3.7%. Treatment with 15 ppm NPs under Cd stress mitigated losses more effectively, with only a 26.9% reduction in chlorophyll a and a 16.9% reduction in carotenoids.

Similarly, Faizan et al.[46] reported reductions in carotenoids (42.2%), total chlorophyll (17.9%), chlorophyll a ([illegible].57%), and chlorophyll b (8.34%), highlighting consistent trends in the negative impact of Cd toxicity on plant pigments. However, CuNP treatment resulted in increased chlorophyll content even in the presence of Cd, indicating a protective role of these nanoparticles in preserving chloroplast integrity and function[47]. This study revealed that Cd stress significantly reduces the stem length and surface area of *T. aestivum*. Under 30 ppm Cd stress, stem length decreased by 28.6%; however, treatment with 20 ppm MA-CuO NPs led to a 23.8% increase. Under severe Cd conditions, 15 ppm MA-CuO NPs mitigated these reductions, highlighting the potential of nanoparticles to increase plant resilience against heavy metal stress.

There are currently no available data on the stem anatomy, stem length, or stem width of *T. aestivum* under varying concentrations of Cd and MA-CuO NPs. Therefore, these parameters were studied in this study to explore their responses to different Cd and MA-CuO NP concentrations. This investigation provides a foundational understanding of how these specific traits are affected by stress conditions, which can help in the formulation of strategies for enhancing plant resilience against heavy metal toxicity through the application of nanotechnology[42,48,49]. The results contribute to a broader knowledge base concerning plant physiology and stress management in agricultural systems. These findings showed that Cd stress significantly impaired the growth of *T. aestivum*. Under 30 ppm Cd stress, spike length decreased from 11.02 cm to 8.37 cm, representing a 24.1% reduction.. The application of 15 ppm MA-CuO NPs maintained the spike length at 13.03 cm (3.9% reduction).

The spikelet count decreased from 12.94 to 12.16 (5.9% reduction), but with 15 ppm MA-CuO NPs, it increased to 13.14 (1.8% reduction). The number of grains decreased from 38.67 to 32 (17.4% reduction), while 15 ppm MA-CuO NPs increased it to 39.45 (2.8% reduction). These results align with those of Alhaithloul et al.[32], who reported that spike length increased by 10%, 18%, 33%, and 46% in various treatments relative to the control. Additionally, their findings revealed that straw yield increased by 19%, 24%, 36%, and 44% at concentrations of 25, 50, 75, and 100 mg/L, respectively. The most significant increase in grain production occurred in the T3 treatment, reflecting a remarkable 43% increase over the control. Similarly, the results of the present study demonstrated that the application of MA-CuO NPs effectively mitigated the adverse effects of Cd stress on the growth of *T. aestivum*. However, their study did not investigate the number of spikelets per spike under Cd stress and MA-CuO NPs[45,48]. Our research specifically examines these parameters under varying concentrations of Cd and MA-CuO NPs, providing valuable insights into their effects on *T. aestivum*. In addition, the literature highlights the importance of exploring spikelet count as a crucial growth metric in the context of heavy metal stress and nanoparticle application.

Biological responses of wheat to green-synthesized CuO NPs under Cd stress were evaluated, revealing promising implications for Cd-stressed crops[15,32]. The findings demonstrate that CuO NPs significantly alleviate Cd toxicity, as evidenced by enhanced plant growth, improved chlorophyll content, and elevated antioxidant enzyme activities[15,50]. These nanoparticles seem to mitigate Cd stress by reducing Cd uptake and translocation within the plant, likely due to CuO NPs-induced changes in the root architecture and cellular barriers which limit Cd entry. Additionally, the enhanced antioxidant enzyme activities, including catalase, superoxide dismutase, and peroxidase, indicate a reduction in oxidative stress, allowing for better physiological functioning of the wheat plants[43,46,48]. Although copper sulfate ($CuSO_4$) is a chemical precursor, the synthesis of CuO NPs in this study is considered biogenic due to the role of plant-derived biomolecules in nanoparticle formation[43]. The *Melia azedarach* leaf extract contains various phytochemicals, including phenolics, flavonoids, and terpenoids, which act as natural reducing and stabilizing agents. These compounds facilitate the conversion of Cu^{2+} ions into CuO NPs without the need for toxic chemical reducing agents, ensuring an eco-friendly and sustainable synthesis approach. This green method enhances the stability and bio-compatibility of the synthesized nanoparticles, making them more suitable for agricultural applications[47,48]. These results suggest that green-synthesized CuO NPs hold potential as a sustainable strategy for improving crop resilience to heavy metal stress, supporting broader adoption in agricultural practices aimed at mitigating soil contamination impacts. Further research may explore optimizing nanoparticle application rates and long-term effects on soil health to ensure environmental safety and crop productivity benefits.

Conclusion

Wheat (*Triticum aestivum* L.) is a cornerstone of global agriculture, valued not only for its adaptability across diverse climates but also for its contribution to human nutrition and economic stability**.** Heavy metal toxicity, particularly from Cd, poses a serious threat to agricultural sustainability by contaminating soils and affecting the food chain. Copper nanoparticles (CuNPs) have the potential to mitigate cadmium stress in *T. aestivum* through the enhancement of antioxidant enzyme activities, which play a critical role in reducing the oxidative damage induced by heavy metal exposure. The wheat variety Arooj-22 was subjected to varying concentrations of $CdCl_2$ (0, 10, 20, and 30 ppm) and MA-CuONPs (0, 10, 15, and 20 ppm). The results revealed that at the highest concentration of 30 ppm Cd, all the morphological, physiological, anatomical, and yield parameters of *T. aestivum* were significantly lower than those of the control group. However, at the highest concentration of MA-CuONPs (20 ppm), a marked increase in all parameters was observed relative to those of the control, indicating the potential of copper nanoparticles in mitigating the adverse effects of Cd toxicity.

Data availability

The datasets used and/or analysed during the current study available from the corresponding author on reasonable request.

Received: 1 November 2024; Accepted: 2 July 2025
Published online: 25 July 2025

References

1. Hossain, M. Z., Bahar, M. M., Sarkar, B., Bolan, N. & Donne, S. fertilizer value of nutrient-enriched biochar and response of canola crop. *J. Soil Sci. Plant Nutr.* **24**, 2123–2137 (2024).
2. Maity, S. & Shrivastav, S. P. understanding heat stress and tolerance mechanisms in wheat (Triticum aestivum L.): A comprehensive review. *J. Adv. Biol. Biotechnol.* **27**, 1196–1211 (2024).
3. Mehmood, S. et al. Impact of different amendments on biochemical responses of sesame (Sesamum indicum L.) plants grown in lead-cadmium contaminated soil. *Plant Physiol. & Biochem.* **132**, 345–355 (2018).
4. Zaheer, M. S. et al. Effect of rhizobacteria and cytokinins application on wheat growth and yield under normal vs drought conditions. *Commun. Soil Sci. Plant Anal.* **50**, 2521–2533 (2019).
5. Zaheer, M. S. et al. Potential effects of biochar application for improving wheat (Triticum aestivum L.) growth and soil biochemical properties under drought stress conditions. *Land* **10**, 1125 (2021).
6. Zaheer, M. S. et al. Inoculation of azospirillum brasilense and exogenous application of trans-zeatin riboside alleviates arsenic induced physiological damages in wheat (Triticum aestivum). *Environ. Sci. Pollut. Res.* **29**, 33909–33919 (2022).
7. Yuan, A. et al. Dynamic interplay among soil nutrients, rhizosphere metabolites, and microbes shape drought and heat stress responses in summer maize. *Soil Biol. Biochem.* **191**, 109357 (2024).
8. Li, X., Zhao, M., Guo, L. & Huang, L. Effect of cadmium on photosynthetic pigments, lipid peroxidation, antioxidants, and artemisinin in hydroponically grown artemisia annua. *J. Environ. Sci.* **24**, 1511–1518 (2012).
9. Jiao, Y., Grant, C. A. & Bailey, L. D. Effects of phosphorus and zinc fertilizer on cadmium uptake and distribution in flax and durum wheat. *J. Sci. Food Agric.* **84**, 777–785 (2004).
10. Sehrish, A. K. et al. Alleviated cadmium toxicity in wheat (Triticum aestivum L.) by the coactive role of zinc oxide nanoparticles and plant growth promoting rhizobacteria on TaEIL1 gene expression, biochemical and physiological changes. *Chemosphere* **364**, 143113 (2024).
11. AL-Huqail, A. A., et al. Evaluation of nanoceria on cadmium uptake in Triticum aestivum (L.) and its implications for dietary health risk. *Chemosphere* **341**, 140115 (2023).

12. Liu, Y. et al. Bacterial social interactions in synthetic *Bacillus* consortia enhance plant growth. *iMeta* https://doi.org/10.1002/imt2.70053 (2025).
13. Sardar, R., Ahmed, S., Shah, A. A. & Yasin, N. A. Selenium nanoparticles reduced cadmium uptake, regulated nutritional homeostasis and antioxidative system in Coriandrum sativum grown in cadmium toxic conditions. *Chemosphere* **287**, 132332 (2022).
14. Umair Hassan, M. et al. Application of zinc oxide nanoparticles to mitigate cadmium toxicity: Mechanisms and future prospects. *Plants* **13**, 1706 (2024).
15. Alaboudi, K. A., Ahmed, B. & Brodie, G. Phytoremediation of Pb and Cd contaminated soils by using sunflower (Helianthus annuus) plant. *Ann. Agric. Sci* **63**, 123–127 (2018).
16. Fathi, A. *et al.* Bioremediation of heavy metals contaminated soils using nanotechnology. In *Bio-organic Amendments for Heavy Metal Remediation* 611–628 (Elsevier). https://doi.org/10.1016/B978-0-443-21610-7.00004-5. (2024)
17. Saqlain Zaheer, M. et al. Exploring the impact of titanium dioxide nanoparticles (nTiO2) at varied concentrations in combination with Azospirillum brasilense on wheat growth and physiology. *J. King Saud. Univ. – Sci.* **36**, 103189 (2024).
18. Alomrani, S. O. et al. Copper nanoparticles alleviate cadmium stress in Solanum melongena through endogenous melatonin and regulation of some physiochemical attributes. *Sci. Hortic.* **323**, 112546 (2024).
19. Inobeme, A. et al. Recent advances in nanotechnology for remediation of heavy metals. *Environ. Monit. Assess.* [illegible], 111 (2023).
20. Shan, C., Dong, K., Wen, D., Cui, Z. & Cao, J. A review of m6A modification in plant development and potential quality improvement. *Int. J. Biol. Macromol.* **308**, 142597 (2025).
21. Soni, S., Jha, A. B., Dubey, R. S. & Sharma, P. Mitigating cadmium accumulation and toxicity in plants: The promising role of nanoparticles. *Sci. Total Environ.* **912**, 168826 (2024).
22. Azarin, K. et al. Impact nano- and micro- form of CdO on barley growth and oxidative stress response. *J. King Saud. Univ. – Sci.* **36**, 103493 (2024).
23. Moradnia, farzaneh *et al.* Green synthesis of nickel oxide nanoparticles using plant extract: An overview of their antibacterial, catalytic, and photocatalytic efficiency in the degradation of organic pollutants. https://doi.org/10.57647/J.IJC.2024.1401.01. (2024)
24. Yang, X. et al. Identification of anthocyanin biosynthesis genes in rice pericarp using PCAMP. *Plant Biotechnol. J.* **17**, 1700–1702 (2019).
25. Shan, C. et al. Writers, readers, and erasers of N6-Methyladenosine (m6A) methylomes in oilseed rape: Identification, molecular evolution, and expression profiling. *BMC Plant Biol.* **25**, 147 (2025).
26. Peng, C. et al. Alginate oligosaccharides trigger multiple defense responses in tobacco and induce resistance to Phytophthora infestans. *Front. Plant Sci.* **16**, 1506873 (2025).
27. Gao, M. et al. Foliar spraying with silicon and selenium reduces cadmium uptake and mitigates cadmium toxicity in rice. *Sci. Total Environ.* **631–632**, 1100–1108 (2018).
28. Vardumyan, H. et al. Additive-mediated phytoextraction of copper-contaminated soils using medicago lupulina L. *Egypt. J. Soil Sci.* **64**, 599–618 (2024).
29. Ghazaryan, K. et al. Soil pollution: An agricultural and environmental problem with nanotechnological remediation opportunities and challenges. *Discov. Sustain.* **5**, 453 (2024).
30. Alhammad, B. A. et al. Effect of co-application of azospirillum brasilense and rhizobium pisi on wheat performance and soil nutrient status under deficit and partial root drying stress. *Plants* **12**, 3141 (2023).
31. FitrianaDyahRatnasari, I. et al. Phytoremediation of cadmium-contaminated soil using terrestrial kale (Ipomoea reptans Poir) and corncob biochar. *J. Degrade. Min. Land Manag.* 7(2), 2318 (2020).
32. Alhaithloul, H. A. S. et al. Effect of green-synthesized copper oxide nanoparticles on growth, physiology, nutrient uptake, and cadmium accumulation in Triticum aestivum (L.). *Ecotoxicol. & Environ. Safety* **268**, 115701 (2023).
33. Ritchie, S. W., Nguyen, H. T. & Holaday, A. S. Leaf water content and gas-exchange parameters of two wheat genotypes differing in drought resistance. *Crop Sci.* **30**, 105–1[illegible] (1990).
34. Allahverdiyev, T. I. Impact of soil water deficit on some physiological parameters of durum and bread wheat genotypes. *AgricultForest* **62**, [illegible] (2016).
35. Arnon, D. I. Copper enzymes in isolated chloroplasts polyphenoloxidase beta vulgaris. *Plant Physiol.* **24**, 1–15 (1949).
36. Chen, Y., Palta, J., Prasad, P. V. V. & Siddique, K. H. M. Phenotypic variability in bread wheat root systems at the early vegetative stage. *BMC Plant Biol.* **20**, 185 (2020).
37. Aslam, M. M., [illegible] & Waseem, M. Cadmium toxicity impacts plant growth and plant remediation strategies. *Plant Growth Regul.* [illegible], 397–412 (2023).
38. Yang, [illegible], [illegible], Zhang, Y., Liu, Y. & Li, H. Wheat morphological and biochemical responses to copper oxide nanoparticles in two soils. *Pedosphere* **34**, 814–825 (2024).
39. Huang, [illegible] et al. Simultaneous exposure of wheat Triticum aestivum L.) to CuO and S nanoparticles alleviates toxicity by reducing Cu accumulation and modulating antioxidant response. *Sci. Total Environ.* **839**, 156285 (2022).
40. [illegible], A., Baruah, K. K., Bhattacharyya, P. & Gorh, D. Integrated nutrient management in wheat grown in a northeast India soil: Impacts on soil organic carbon fractions in relation to grain yield. *Soil & Tillage Res.* **168**, 81–91 (2017).
41. [illegible]za, M. A. S. et al. Cu-nanoparticles enhance the sustainable growth and yield of drought-subjected wheat through physiological progress. *Sci. Rep.* **14**, 14254 (2024).
42. Noman, M. et al. Biogenic copper nanoparticles synthesized by using a copper-resistant strain Shigella flexneri SNT22 reduced the translocation of cadmium from soil to wheat plants. *J. Hazard. Mater.* **398**, 123175 (2020).
43. Ahmed, S. F. et al. Green approaches in synthesising nanomaterials for environmental nanobioremediation: Technological advancements, applications, benefits and challenges. *Environ. Res.* **204**, 111967 (2022).
44. Rehman, A. et al. Exploring the nano-wonders: unveiling the role of Nanoparticles in enhancing salinity and drought tolerance in plants. *Front. Plant Sci.* **14**, 1324176 (2024).
45. Ibrahim, A. S., Ali, G. A. M., Hassanein, A., Attia, A. M. & Marzouk, E. R. Toxicity and uptake of CuO nanoparticles: Evaluation of an emerging nanofertilizer on wheat (Triticum aestivum L.) plant. *Sustainability* **14**, 4914 (2022).
46. Faizan, M. et al. Nanoparticle mediated plant tolerance to heavy metal stress: What we know?. *Sustainability* **15**, 1446 (2023).
47. Muradoglu, F. et al. Cadmium toxicity affects chlorophyll a and b content, antioxidant enzyme activities and mineral nutrient accumulation in strawberry. *Biol. Res.* **48**, 11 (2015).
48. Nawaz, A. et al. Nanobiotechnology in crop stress management: an overview of novel applications. *Discov. Nano* **18**, 74 (2023).
49. Huang, X. et al. Application of cyclopropane with triangular stable structure in pesticides. *J. Mol. Struct.* **1326**, 141171 (2025).
50. Han, Y. et al. Improving aerobic digestion of food waste by adding a personalized microbial inoculum. *Curr. Microbiol.* **81**, 277 (2024).

Acknowledgements

The authors appreciate the support provided by Ongoing Research Funding Program (ORF-2025-708), King Saud University, Riyadh, Saudi Arabia.

Author contributions

Conceptualization, M. and I.N.; methodology, A.A.C., A.R.; software, I.A.; validation, W.H.; formal analysis, I.N.; investigation, M. and I.N.; resources, I.A.; data curation, M.; writing-original draft preparation, A.A.C., M., I.N., I.A., A.R., W.H., and M.W.R.; writing-review and editing, M.S.Z., M.R., S.M.; visualization, M.; supervision, M. and A.A.C.; project administration, M.; funding acquisition, M.R. and M.S.Z. All authors have read and agreed to the published version of the manuscript.

Funding

Open Access funding enabled and organized by Projekt DEAL.

Declarations

Competing interests

The authors declare no competing interests.

Ethics approval

All local, national or international guidelines and legislation were adhered to for the use of plants in this study.

Declaration of Generative AI and AI-assisted technologies in the writing process

During the preparation of this manuscript the author(s) used Chat GPT and Grammarly in order to improve the technical and English language of the paper. After using this tool/service, the author(s) reviewed and edited the content as needed and take(s) full responsibility for the content of the publication.

Additional information

Correspondence and requests for materials should be addressed to M., A.A.C., M.S.Z. or M.R.